MBE GROWTH AND INITIAL NUCLEATION KINETICS

OF GaN ON GaAs (100) SUBSTRATES

By

MARK LEE O'STEEN

Bachelor of Science

Southeastern Oklahoma State University
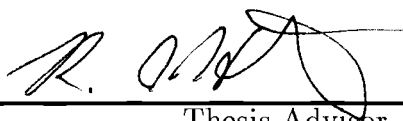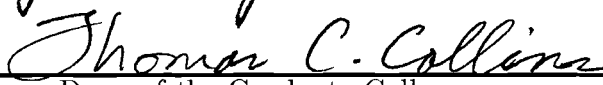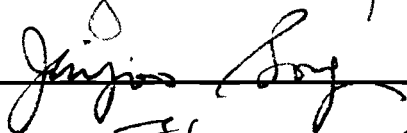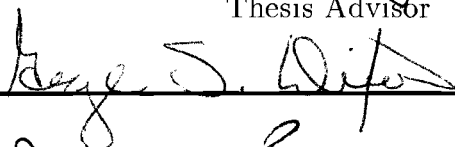
Durant, Oklahoma

1993

MBE GROWTH AND INITITIAL NUCLEATION KINETICS

OF GaN ON GaAs (100) SUBSTRATES

Thesis Approved:

_____
Thesis Advisor

_____

_____

_____
Dean of the Graduate College

ACKNOWLEDGMENTS

The credit for the good things in this document should be shared by all that had a hand in it; each in some way made a major contribution. However, the credit for the inconsistencies found within should be entirely mine. There are many people that I must thank for their contribution to this thesis. First and foremost, I must thank my advisor, Dr. R. J. Hauenstein; his patience and tolerance with me, especially during the writing of this thesis, has been unending. Furthermore, his keen insight has driven this project from the onset. Also, I must thank Drs. J. J. Song and G. S. Dixon for serving as members of my thesis committee. Their diligent reading has made this a better document and me a sharper thinker.

Next, I must acknowledge my collaborators in this project: Zvonomir Bandić, and Drs. D. A. Collins and T. C. McGill, each of the California Institute of Technology. They have provided the HRXRD data and some of the digital RHEED data. Furthermore, their intellectual input has been most helpful in the science of this study. I would like to thank Dr. S. J. Hwang, of Oklahoma State University for assisting in the growth of the samples for this study and Dr. J. J. Song for allowing him to neglect his own work to do so. I have also benefited from collaboration with Dr. R. M. Feenstra of Carnegie Mellon University.* While his cross-sectional STM studies of the samples grown in this study are still underway, his esteemed input has been helpful in confirming some of the principle conclusions of this thesis. Also, I need to thank both Les Colyott and Xiaoping Cai for their very fundamental contributions to this project. Without their efforts, this project would have been much longer in arriving.

Furthermore, I need to thank Ulf Nobbman, and Dr. Brian Markey for donating the LaTeX files for their theses; they have saved me many hours of re-inventing

*formerly with the IBM Thomas J. Watson Research Center.

iii

the same "$\LaTeX$" wheels. Next, I need to thank all of the remaining faculty, staff, and students of the Physics department. Each has served, at some point, to explain something to me, to redirect me when I have gone astray, or simply to encourage me when the MBE system was so frequently down. Also, I would like to thank Dr. W. J. Polson of Southeastern Oklahoma State University for getting me into Physics in the first place back when I thought Math would be a really cool major. Finally, I would like to thank my family, my parents in particular, and my friends who have encouraged me to always move forward at the speed of my own ambition.

TABLE OF CONTENTS

LIST OF TABLES

LIST OF FIGURES

CHAPTER 1

INTRODUCTION

1.1   INTRODUCTION

Society's addiction to technology is readily apparent. Along with the prolif-
eration of electronics into our daily lives, there has also come a continuing need
for improvements to the basic electronic devices that are used in the electronic
equipment that surrounds us. Not only is there a need to improve current devices
but also a constant struggle to develop new electronic devices to serve in applic-
ations for which there is currently no suitable technology. This need to develop
new and improved technological devices has led to many extensive studies of semi-
conducting materials. One material that has been the subject of intense study as of
late is Gallium Nitride (GaN). This thesis will deal with the very important initial
nucleation of GaN growth and the growth of GaN by Molecular Beam Epitaxy.

Recently, a great deal of research has been performed in hopes of developing
materials suitable for fabricating Light Emitting Diodes(LED) and laser diodes in
the ultraviolet to blue-green region of the electro-magnetic spectrum. There are a
number of reasons why these devices are of interest. A few of these reasons include
the following: (1) Replacement of red and infra-red LED's in optical storage devices,
such a CD-ROM's, could provide a factor of 10 increase in the storage capacity of
such devices;[1] (2) Solid state laser diodes could serve as a stable and economical
alternative to gas lasers operating in the same region of the optical spectrum;[1]
(3) Laser diodes in the blue region of the spectrum could be used to improve the
speed of laser printers by one or two orders of magnitude by allowing the use of
more sensitive photoconducting materials and are anticipated to make high quality
color laser printers inexpensive as well.[1]

Fortunately, there are materials that exhibit enormous potential for use in the manufacturing of such devices; two of the most important are Gallium Nitride (GaN) and Zinc Selenide (ZnSe). While blue LED's have already been manufactured using both materials,[2,3] GaN is being pursued quite actively. This is due, in part, to the desirable properties of mechanical rigidity and thermal stability that GaN offers.[4]

Until the recent onset of research in the search for a blue LED, GaN had remained relatively unexplored; this was due to the relative difficulty associated with attaining bulk GaN in suitable quantity and quality for study.[4] Advances in the technology of plasma sources for generating ionized and excited nitrogen species has made several variations of Molecular Beam Epitaxy (MBE) viable processes by which high quality GaN can be grown. Each of the MBE processes used to grow GaN involves the inclusion of some type of reactor to ionize and excite the nitrogen source gas used in the growth process.

For this thesis, both the growth of epitaxial GaN films and the initial nucleation of GaN growth on GaAs (100) substrates have been studied in qualitative and quantitative detail. The specific process by which GaN was grown for this study is known as Electron Cyclotron Resonance Plasma-Assisted Molecular Beam Epitaxy (ECR-MBE). Both *in situ* and *ex situ* characterizations are used in this study. The primary *ex situ* characterization for this study was High Resolution X-Ray Diffraction (HRXRD); this was used primarily for making structural and compositional characterizations of the samples. The *in situ* characterizations are primarily Reflection High Energy Electron Diffraction (RHEED) and indirectly Quadrapole Mass Spectroscopy (QMS); these are used respectively to characterize the surfaces of the samples grown and, in the case of GaAs growth, to characterize the growth chamber environment.

The outline of this thesis will be as follows. Chapter 1 will introduce most of the background material associated with the growth and the theory of the various characterizations that are used. Chapter 2 will be concerned with an early set of growth experiments aimed at simply producing epitaxial GaN on GaAs (100)

substrates. As will be discussed in Chapter 2, there are some interesting physical phenomena observed in the initial nucleation of GaN growth on GaAs (100). Necessarily, a detailed study of these phenomena was undertaken. This study of the initial nucleation of growth and surface interaction will be the subject of Chapter 3. Finally, Chapter 4 will summarize the material presented. Also included (as appendices) will be information concerning the retrofit and upgrade of the MBE system used for the work at hand, and the preparation procedures for samples. This is included for its informative value, but mainly for the purpose of making a permanent historical record for future generations of graduate students who will, no doubt, be very concerned with this information.

Now, to proceed further, a brief outline of the remaining portion of Chapter 1 is necessary. Section 1.2 will deal generally with MBE, using GaAs as a recurrent example, and specifically with ECR-MBE for the growth of GaN. Section 1.3 will be dedicated to the theory and application of the various characterizations that are made of the samples in this study. First will be the *in situ* characterizations, RHEED and QMS. Second will be the *ex situ* characterization, HRXRD. Finally, Section 1.4 will outline briefly what has been accomplished through this research and the importance of this work.

1.2 MOLECULAR BEAM EPITAXY

1.2.1 CONVENTIONAL MBE

As has already been touched upon, there are several variations of MBE. For this section of the thesis, where the concern is the MBE process in general, the focus shall be restricted to conventional or solid-source Molecular Beam Epitaxy. The restriction being placed is simply that the molecular beams are produced by conventional solid-source cells and crackers.

Molecular Beam Epitaxy is a modern technique used to grow epitaxial thin films on crystalline substrates. Typically, the crystals grown by MBE are semiconductors. While there are a number of variations on the basic MBE process, all

crystals—when grown properly—will exhibit a number of common characteristics. First, the crystals grown by molecular beam epitaxy are epitaxial. In this context, the term epitaxial will imply that the films which are grown are crystallographically commensurate with the underlying substrate or epilayers upon which they are deposited.[5,6] Second, crystals grown by MBE are typically very thin; hence they are referred to as thin films. Most samples grown by MBE will not exceed more than a few microns in total thickness. Furthermore, the films grown by MBE are found to be of very high quality when compared to thin films grown by other growth techniques.[6] Finally, the thin films grown by molecular beam epitaxy can be controlled to a very high degree of precision; submonolayer resolution is readily attained.[5]

The fundamentals on the MBE growth process are quite simple. In MBE, molecular beams are generated by sources of some type—typically effusion cells—and are incident upon a heated, monocrystalline substrate. At the surface of the substrate, the molecular beams "stick" with some efficiency. Since more than one beam is incident at the surface, the materials react, forming bonds, and become incorporated into the sample surface. The substrate is kept at a temperature that is sufficiently high so as to give the incident materials enough thermal energy to be mobile, but not so much thermal energy as to vigorously re-evaporate the materials. Since the deposited material has sufficient energy to be mobile, the point on the lattice at which the material is incorporated is not completely random. As is required by thermodynamics, the deposited material will find the location which minimizes the free energy of the total system.[5,7] In an effort to reduce the free energy, the atoms at the terminating surface of the sample will reconstruct to eliminate dangling bonds. However, the atoms in the reconstructed surface are in a higher energy state than the non-reconstructed atoms within the bulk of the crystal. Therefore, thermodynamics requires that there be a minimum amount of surface in order to minimize the free energy of the system. Thus, the deposited material will form a surface that is extremely flat on the atomic scale. As material is deposited

in this way, the monocrystalline substrate "grows". To see the geometry of a MBE system, refer to Fig. 1.1 on p. 6.

Clearly, the rate of the growth of the crystal is dependent on the flux rates of the materials onto the substrate and the efficiency at which the materials stick to the substrate. Little can be done to control the efficiency at which the materials stick to the substrate, other than adjusting the temperature of the substrate, which consequently affects the mobility of the materials deposited on the surface. Alternatively, the flux rates of material onto the substrates can be and are readily controlled. This is facilitated by controlling the temperature of the cells used to evaporate (or sublimate) the materials used in growth and by using mechanical shutters at the orifice of each cell. The cells that are used in conventional MBE are referred to as effusion cells, K-cells, and on occasion as Knudsen cells.[5] Each cell is essentially a pyrolytic Boron Nitride crucible encased by a Tantalum wire heater and in direct contact with a thermocouple; refer to Fig. 1.2 on p. 7. Each material that is to be deposited is placed inside the Boron Nitride crucible of an effusion cell. The tantalum wire heater is powered by an external supply, which is controlled through a feedback loop using the thermocouple of the effusion cell and a process control computer.

It is necessary that MBE samples be grown in an Ultra-High Vacuum (UHV) chamber. This vacuum condition is necessary for two reasons: (1) to ensure that the mean-free path of the evaporated or sublimated source materials is sufficiently large so that the materials reach the heated substrate without being significantly scattered; (2) to ensure that other unwanted materials that could become incorporated into the film are not present. Such materials, when incorporated, lower the quality of the film and may act as dopants.

To give a more realistic impression of MBE growth of samples, it is instructive to consider the growth of GaAs which is a material that can readily be grown by MBE. The important parameters to control in the MBE growth of GaAs are (1) the substrate temperature, (2) the Ga flux, and (3) the ratio of As_2 to Ga. Typically, GaAs is grown at temperatures near 600°C. It is not uncommon, however, to see

Heater

Sample

Ultrahigh Vacuum Chamber

Shutters
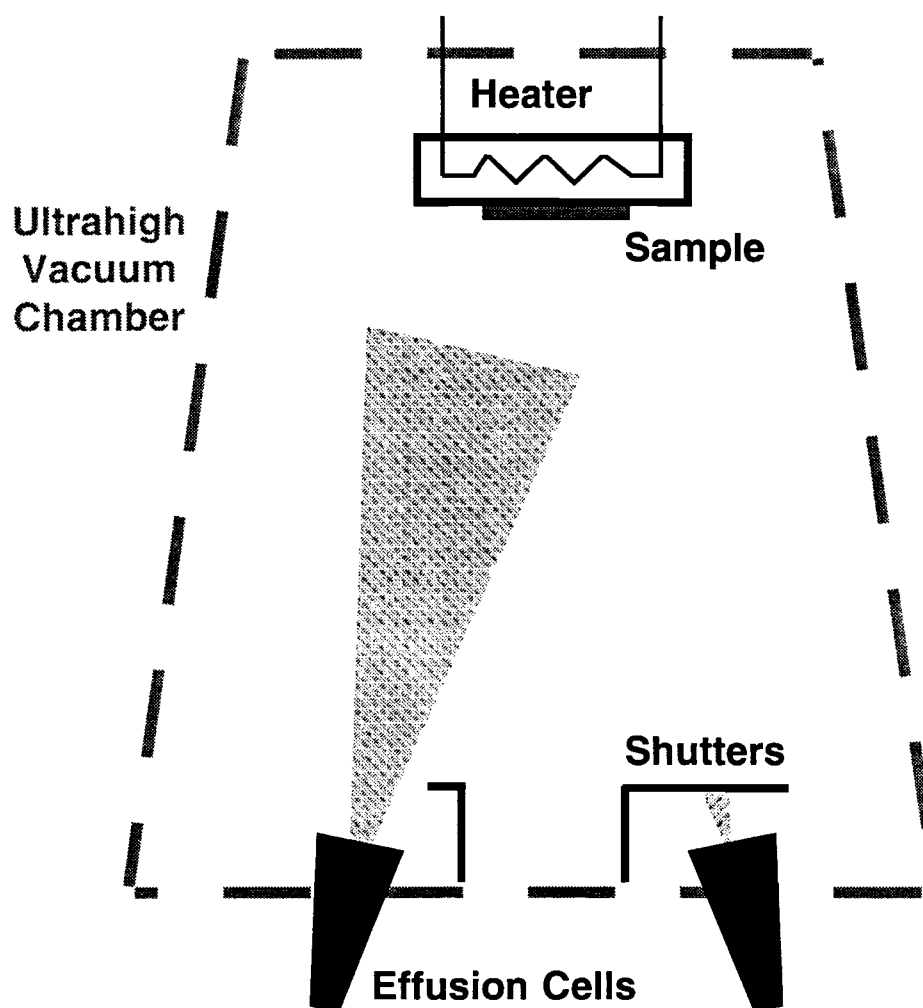
Effusion Cells

Figure 1.1. Schematic representation of a general Molecular Beam Epitaxy system.

Boron Nitride Crucible

Tantalum Wire Heater

Power Supply

Source Material

Process Control PC
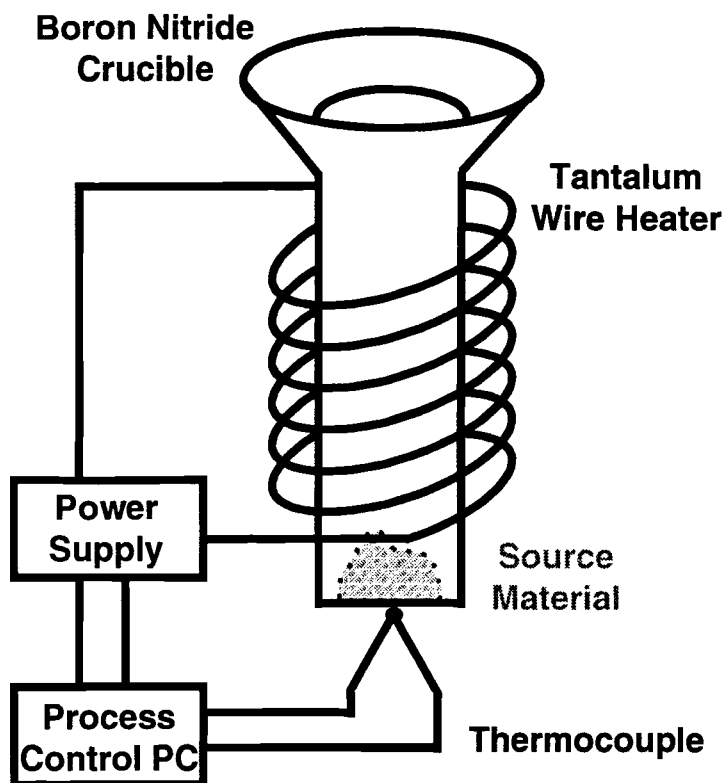
Thermocouple

Figure 1.2. Shown schematically is an effusion or K-cell used to generate molecular beams for growth. The thermocouple is used by process control computers to regulate the external power supply and consequently the temperature of the effusion cell.

samples grown as low as 400°C; such samples usually are higher in defects due to the lack of mobility of atoms at the surface during growth. Amazingly, epitaxial growth on a reconstructed GaAs surface has been reported at temperatures as low as 257°C.[8,9]

The fluxes of Ga and As during growth are practically independent of the "sticking coefficients" that were alluded to earlier. For the case of a Ga flux onto a substrate at typical growth temperatures, the "sticking coefficient" is, for all intents and purposes 1, or 100%.[5,6] The necessary flux of As is not determined merely by the desired growth rate. For GaAs at typical growth temperatures, As is preferentially evaporated from the surface of the sample. In order to maintain the stoichiometry of the sample, it is necessary to have an overpressure of As to compensate for As evaporated from the surface and near surface layers. The overpressure of As serves both to provide the As flux necessary for growth as well as the As necessary to preserve the surface stoichiometry. When the necessary overpressure of As is present, the sample being grown is described as having an "As-stabilized" surface.[5,6] The lack of a sufficient overpressure of As will result in a "Ga-stabilized" surface.[5,6] These are very important concepts in MBE growth and consequently of this thesis. These concepts will be addressed again in Chapter 3.

The overpressure of As required to maintain the As-stabilized surface depends on the temperature of the substrate.[5,6] At typical temperatures (near 600°C) during the deposition at normal rates, a 1.8:1 to 3:1 ratio of As_2 to Ga is necessary; however, at elevated temperatures, a 50:1 ratio may be needed.[5] Note that when speaking from a practical standpoint, partial pressures or beam-equivalent pressures are discussed rather than fluxes as these are the quantities that are easily measured within the growth chamber.

Once the various components of the MBE system are placed in a state appropriate for growth, the growth of GaAs is modulated simply by opening and closing the mechanical shutter in front of the Ga effusion cell. Closing the shutter assures that the heated Ga within the effusion cell is no longer "line of sight" with the substrate and this effectively eliminates the beam of Ga. It is necessary that the

As shutter always remain open while the substrate is at high temperatures in order to maintain the As overpressure used to preserve the As-stabilized surface.

Typical growth rates for GaAs deposition are approximately 1 monolayer/sec (ML/sec) or less. While it is possible to grow at rates of 10 ML/sec, there is a tradeoff between the quality of the sample and the expediency of the growth.[5] To achieve a growth rate of 1 ML/sec, it is necessary to have an As_2 partial pressure of approximately 1.0×10^{-6} Torr.[5,6]

1.2.2   ECR-MBE

All the GaN samples grown in this study were grown by a very specific type of MBE called Electron Cyclotron Resonance Plasma-Assisted Molecular Beam Epitaxy (ECR-MBE). This growth process is virtually identical to that of conventional MBE with the exception of a few very subtle differences. The principal differences are (1) a gas source and plasma reactor are used in lieu of a conventional effusion cell, and (2) samples are grown at an exceptionally high pressure in order to maintain conditions suitable to the operation of the plasma reactor.

The Electron Cyclotron Resonance Plasma Reactor is straightforward in its design. Radically different from the conventional effusion cells, the ECR Plasma Reactor allows a controlled leak of a gas, diatomic nitrogen in this case, radially into the side of a small alumina cup, referred to as the plasma cup. The opening of this cup is pointed toward the position of the sample in the MBE growth chamber; also, this opening may be covered, but not sealed, by a mechanical shutter identical to those used in conventional MBE. Microwaves are focused onto the interior of the plasma cup by a small antenna on a sliding metal contact. This metal contact, which adjoins the antenna to a waveguide, is adjusted to optimize the resonance cavity. Finally, the plasma cup is located within a group of magnetic rings. These magnetic rings are assembled with common poles facing each other. This produces a static magnetic field designed to retain electrons within the plasma cup and to shape the beam of ionized nitrogen leaving the plasma cup. Refer to Fig. 1.3 on p. 10 for a diagram of this component.
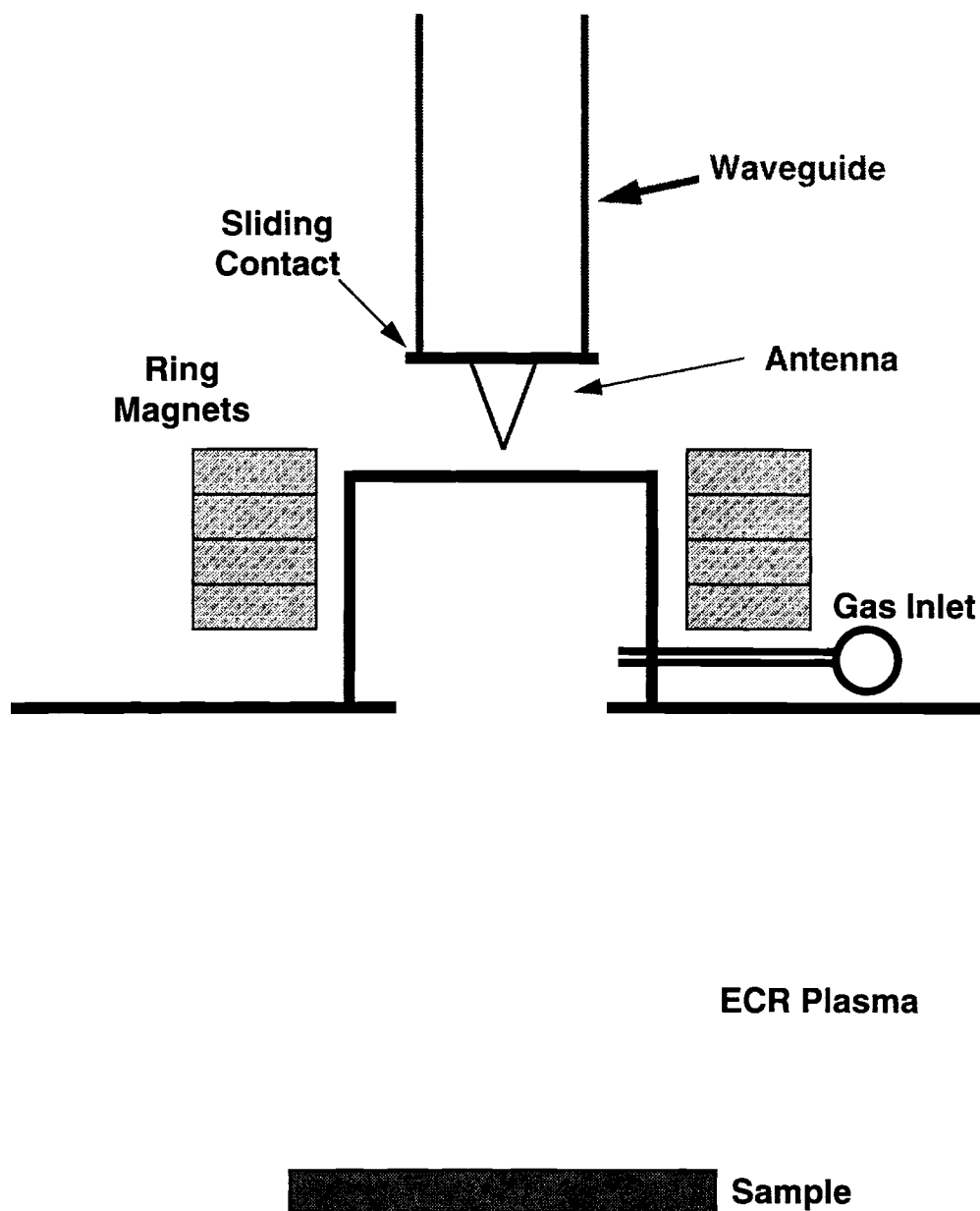
Figure 1.3. Represented is the Electron Cyclotron Resonance Plasma Reactor used in the growth of GaN and in the surface nitridation experiments.

The microwaves are generated by an external source at a specific frequency. This frequency is chosen to match the natural cyclotron frequency of the electron gas in the presence of the magnetic field. The cyclotron frequency is simply related to the magnetic field B by:

$$\omega_{ce} = \frac{eB}{m_e} \tag{1.1}$$

where in Eq. (1.1) ω_{ce} is the cyclotron frequency, e and m_e are respectively the mass and charge of the electron, and B is the magnetic field strength.[10] Under the forces due to the static magnetic field and due to the incident flux of microwaves, the electrons are accelerated through a helical path with increasing radius. Individual electrons readily reach energies of 10 to 20 eV.[10] Upon collision with gases in the plasma cup, excited and ionized species are generated. These ionized and excited species leave through the opening in front of the plasma cup. With a sufficient power of incident microwaves and sufficient nitrogen in the plasma cup, a nitrogen plasma can be generated.

The specific ECR Plasma Reactor used in this study was designed to operate from 10^{-5} Torr to 10^{-2} Torr.[11] These higher pressures have proven to be necessary so that the ECR Plasma can be established and controlled repeatably. Unfortunately, these pressures are a minimum of a factor of 10 greater than the normal pressures at which GaAs is normally grown. As was already pointed out, ECR-MBE is conducted at pressures much greater than ordinary MBE. The principal problem with this is that the higher pressures imply a shorter mean free path for the materials in the molecular beams. Effectively, the flux of material from the source cells is attenuated due to scattering at the higher pressures. In principle, this can be compensated for by increasing the flux of material or by allowing a longer period of growth at slower rates.

1.3 CHARACTERIZATIONS OF EPITAXIAL MATERIALS

1.3.1 *IN SITU* CHARACTERIZATION

1.3.1.1 REFLECTION HIGH ENERGY ELECTRON DIFFRACTION.

While in the process of growing samples by either conventional MBE or ECR-MBE, it is useful to have information concerning the structure of the sample immediately available to the grower. Arguably, the most important *in situ* characterization of MBE grown samples is Reflection High Energy Electron Diffraction (RHEED). RHEED is a simple and immediate characterization that will, by imaging the surface in reciprocal space, provide much detailed information about the structure of the sample surface.[5,12,13]

In characterizing samples by RHEED, a monoenergetic beam of high energy electrons (5 to 50 keV) is made incident on the surface of the sample at a grazing angle ($< 2\deg$).[5,14] As the electrons have a wave nature and the sample is monocrystalline, the beam of electrons will be diffracted as if from a grating. The geometry of the experiment is shown in Fig. 1.4 on p. 13.

To understand the diffraction patterns that are attained, it is easiest to employ the Ewald Construction. First, since GaAs is a face centered cubic structure, the magnitude of the shortest reciprocal lattice vector at the surface is given by $k = 2\sqrt{2}\pi/a_0^{\mathrm{GaAs}}$ where a_0^{GaAs} is the lattice parameter of GaAs (5.65 Å for unreconstructed GaAs[15,14]). This implies that $k = 1.57\text{Å}^{-1}$. Next, the radius of the Ewald sphere will largely depend on the accelerating voltage. The de Broglie wavelength is found as:

$$\lambda = \left[\frac{h^2}{2m_e eV \left(1 + \frac{eV}{2m_e c^2}\right)} \right]^{\frac{1}{2}} \qquad (1.2)$$

where in Eq. (1.2) h is Planck's constant, m_e and e are respectively the rest mass and the charge of the electron, c is the speed of light in a vacuum, and V is the potential difference through which the electrons are accelerated.[5,16,17] This relationship can be derived by a straightforward application of special relativity. From this, the radius of the Ewald sphere is $2\pi/\lambda \approx 52\text{Å}^{-1}$ for the case of 10 keV electrons.
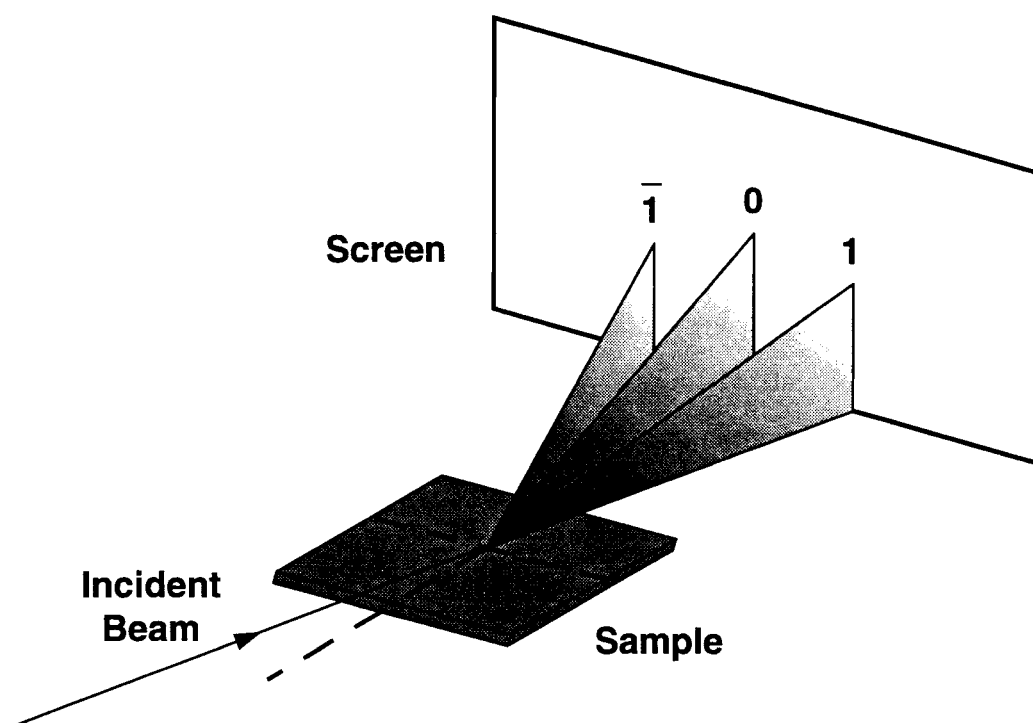
Figure 1.4. Schematic representation of the geometry of Reflection High Energy Electron Diffraction.

Further, the lattice points at the surface of the sample will be rods perpendicular to the plane of the substrate in reciprocal lattice space. These rods will have some width due to thermal vibrations.[5] Also, the Ewald Sphere will have some thickness associated with it also due to variations in the energy of the electrons.[5] The allowed reflections will be given by the intersections of the Ewald sphere with the rods in reciprocal space. The intersections can most easily been seen by considering Fig. 1.5 on p. 15. Since the radius of the Ewald sphere is many times greater than the shortest reciprocal lattice vector, the intersection of the Ewald sphere and rods principally produces streaks rather than spots.

As it is essential to understanding much of this thesis, the basic notation used in referring to RHEED patterns needs to be presented. It was pointed out earlier that the surface of a sample will reconstruct to eliminate dangling bonds in an effort to reduce the free energy. Reconstruction of the surface causes the formation of a periodic surface cell or a periodic mesh. The period of this surface cell will be different from that of the underlying material. Typically, the unit mesh of such a surface cell is described as an $(n \times m)$ surface reconstruction. This notation implies that surface reconstruction cell is n times larger than the unit cell of the underlying material along one principal axis, and m times larger along the other principle axis. Implicitly, the third principal axis is orthogonal to the growth surface.

The size of the surface reconstruction cell as compared to that of the underlying bulk cell can be directly observed through RHEED. The presence of a structure at the surface that is n times the size of the underlying cell implies that there will be additional rods in reciprocal space that are separated by 1/n times the normal spacing of the underlying material. These additional rods will allow 1/n-th order diffraction lines to be observed in the RHEED patterns. Such lines are so commonly observed, that RHEED patterns are referred to by these additional diffraction lines.

The surface of a GaAs sample under typical growth conditions exhibits a (2×4) surface reconstruction (pronounced "two by four"). In this notation, the
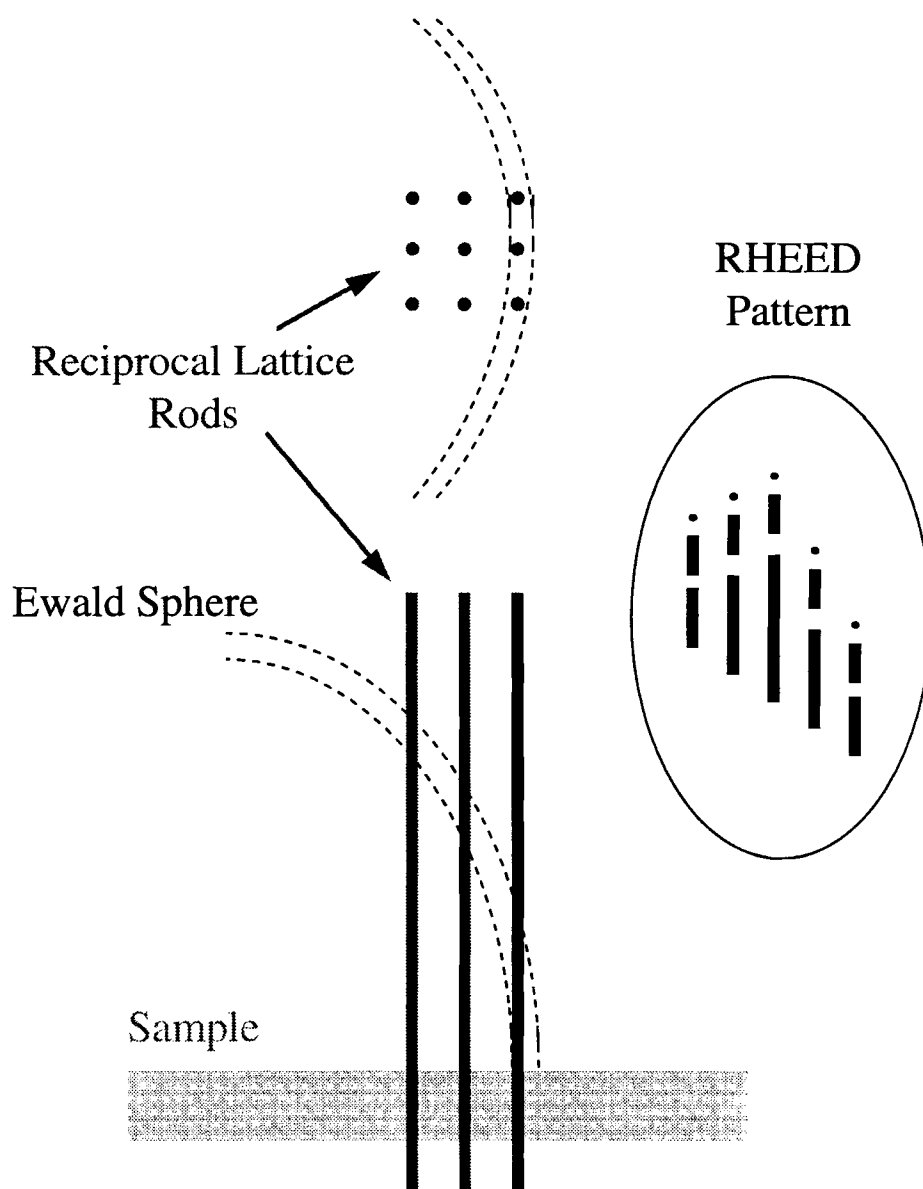
Figure 1.5. Schematic illustration of the Ewald Construction for RHEED. Illustrated are the intersections of the rods in reciprocal space with the Ewald sphere.

first number refers to the RHEED pattern observed along the sample [110] direction and the second number refers to the RHEED pattern observed in the [1$\bar{1}$0] direction. The individual patterns observed along the [110] and [1$\bar{1}$0] directions are referred to as 2× and 4× (pronounced "two by" and "four by") reconstruction patterns, respectively. In this thesis, references will be made to a number of surface reconstruction patterns. Some of these include (2 × 2)'s, (2 × 4)'s, and (3 × 3)'s. To determine that these reconstruction patterns existed, it was necessary to see the appropriate pairs of 2×, 3×, and 4× RHEED patterns along the [110] and [1$\bar{1}$0] directions.

A very interesting phenomenon that is observed at the initiation of the MBE growth of epitaxial films is RHEED oscillations.[5] In RHEED oscillations, a periodic oscillation of the intensity of RHEED streaks is observed at the onset of deposition of GaAs on a high quality surface. The oscillatory component of the RHEED streak intensity is observed to decay exponentially in time. The study of RHEED oscillations is fundamentally important; as will be argued, the period of the oscillation of the intensity of the RHEED patterns exactly corresponds to the growth of one epitaxial monolayer.[5] Measuring the period of RHEED oscillations is the simplest method of attaining growth rates accurately. Ideally, before growth is initiated, the sample surface is very flat, even on the atomic scale. As material is deposited, it grows in the fashion that was described earlier. However, it was not mentioned at that time that the deposited material tends to form into islands that grow together with the further deposition of material.[5] Thus, it is expected that the greatest RHEED intensity would occur when the surface is flattest and the least intensity would occur when the surface is most divided into islands. This island growth can be seen in Fig. 1.6 on p. 17. The period of the fluctuation of the intensity of the RHEED pattern then directly corresponds to the growth of one monolayer of material. The decay of the overall intensity of the pattern is due to the roughness of the surface that develops during the growth of epilayers.[5] During growth, the surface will come to some working equilibrium of roughness. As the
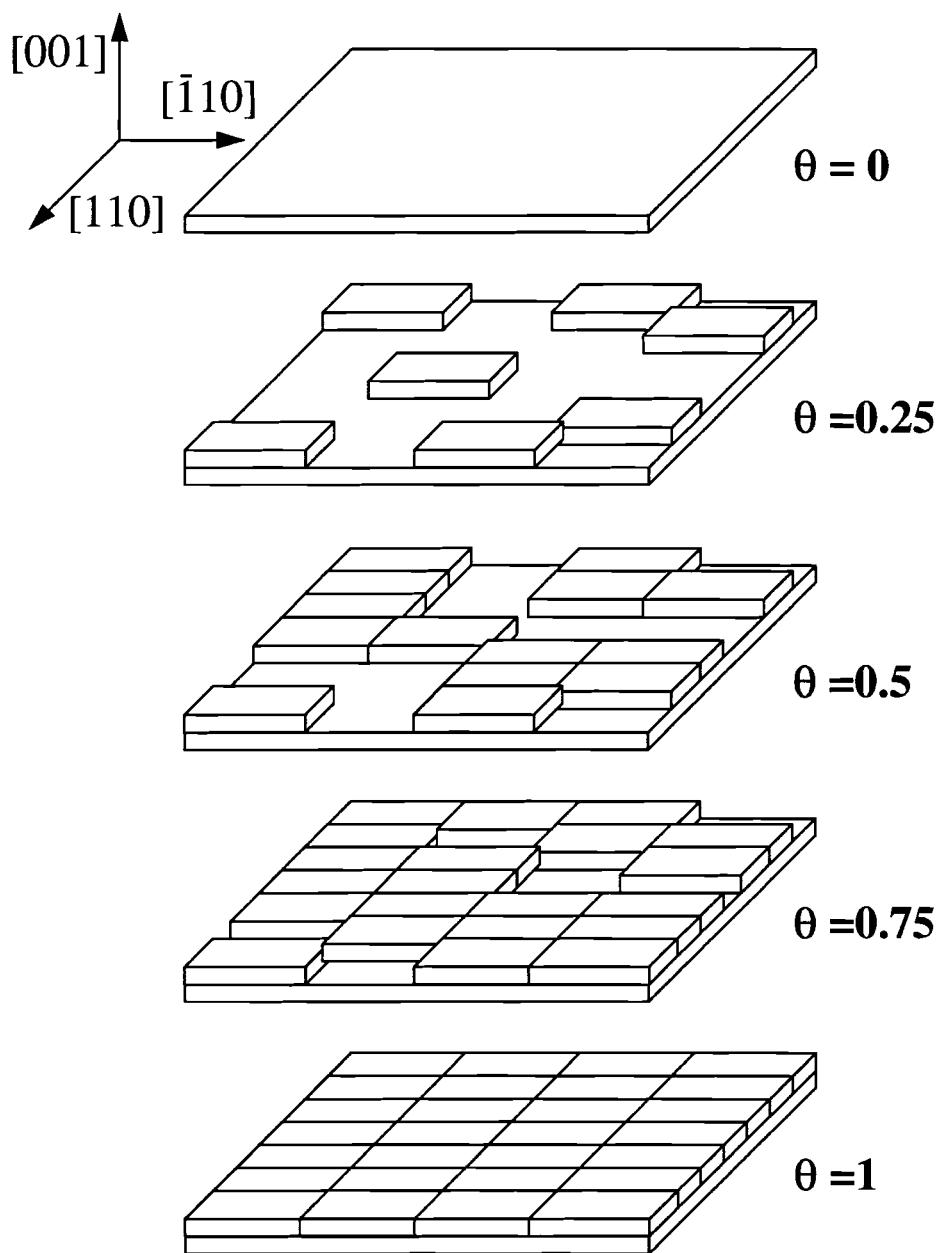
Figure 1.6. Schematic representation of epilayer growth through the coalescence of island-like structures. Θ represents the fractional surface coverage of a single GaAs layer.

surface is not as flat, there is a corresponding loss of intensity in the RHEED pattern. Once the growth is interrupted, the surface will relax and form the flattest possible surface as is required to minimize the free energy of the aggregate system.

It is further worth noting that in the case of GaAs growth, RHEED oscillations are most easily seen in the [110] direction. It is believed that this is due to preferential ordering along this direction causing reflections from this azimuth to be most strongly affected by the formation of islands.[5]

1.3.1.2 QUADRAPOLE MASS SPECTROMETRY. Another very important analytical tool that is used in the growth of epitaxial samples by MBE is the Quadrapole Mass Spectrometer (QMS), more commonly referred to as the Residual Gas Analyzer (RGA). The RGA does not directly characterize the samples that are grown, but is important because it characterizes the environment in which the samples are grown. For this reason, the RGA is an important resource during the growth of an epitaxial sample. Unfortunately, because of the limited operating range of pressures for the RGA, it is only useful during the growth of GaAs. For the growth of GaN, the RGA must effectively be turned off.

The RGA consists of three main parts: the ion source or ionizer, the analyzer or ion filter, and the ion detector.[18] The ionizer consists of a thoriated iridium filament encased within grids or meshes that are each electrically isolated. When heated, the filament emits electrons which are accelerated by the various grids of the ionizer. These electrons may strike and ionize any of the atoms or molecules of the gases within the ionizer. Once ionized, the atoms and molecules are accelerated to the center most portion of the ionizer. From this area, ions are periodically accelerated into the analyzer by a 500 Hz square wave potential.

The analyzer consists of four parallel rods or poles. Each of the rods is electrically connected to the rod diametrically located to itself. These four rods form a quadrapole. Ions are accelerated along the length of these rods into the ion detector. One pair of the quadrapole rods is biased with a positive dc potential. This serves the purpose of filtering ions that have a mass to charge ratio which is

too large. The second pair of quadrapole rods is biased with an RF signal. This pair of rods serves the purpose of filtering ions which have too small of a mass to charge ratio. The charge to mass ratio that survives the filter and the selectivity of the filter are determined by appropriate choices of the amplitudes of the signals on the quadrapole rods and the frequency of the RF signal.

Ions that survive the analyzer enter the ion detector. The ion detector is composed of two parts: the electron multiplier and the Faraday cup. The Faraday cup is simply a plate used to discharge ionized species that strike it. The current from this plate is taken as the signal to the computer processors. As this current can be quite low under ultra-high vacuum conditions, it is necessary to have an Electron Multiplier before the Faraday Cup to act as a preamplifier. The Electron Multiplier has operating voltages ranging from -1 to -3 kV. Thus, ionized species reach it with substantial energy. Upon striking the surface, secondary electrons are emitted which are accelerated along the length of the Electron Multiplier and eventually to the Faraday Cup, thus increasing the signal.

1.3.2 *EX SITU* CHARACTERIZATION

The only *ex situ* characterization that was performed on the samples grown that will be discussed in detail in this work is High Resolution X-Ray Diffraction. In this section, the experimental details of the X-Ray Diffraction experiment will be presented along with a basic procedure for analyzing the data attained for superlattice samples.

The primary measurement made using X-Ray Diffraction was the $\Omega/2\theta$ style Rocking curve. In this approach, a highly collimated beam of x-rays is generated through the use of a 4-crystal monochromator and an X-Ray source. In this specific case, the X-Ray source utilized the Cu K-α_1 emission line and the 4-Crystal monochromator used (220) reflections from Germanium crystals. The X-Rays are incident at an angle Ω, which is near the Bragg angle. The detector used in the measurement has a fine entrance slit and is kept at an angle θ relative to the substrate. Since reflections from the (400) planes are observed, θ and Ω will ideally be

kept equal throughout data acquisition. From this, the angle between the detector and the incident beam of X-Rays is basically 2θ. Refer to Fig. 1.7 on p. 21. The data is acquired as both the detector and the sample are rotated with the detector rotating at twice the angular speed. The data acquired in this experimental scheme is referred to as an $\Omega/2\theta$ "Rocking Curve".[19-21]

It is worthwhile to discuss at this point the analysis of the Rocking Curves that are attained. For the work presented in Chapter 3, it was necessary to grow $GaN_yAs_{1-y}/GaAs$ superlattice structures. These samples were composed of 36 periods of a GaN_yAs_{1-y} monolayer overgrown with an approximately 220 Å GaAs layer. The rationale for growing such a structure will be discussed in Chapter 3. X-Ray Diffraction measurements were used to determine the monolayer equivalent incorporation of nitrogen, y. A typical Rocking Curve attained from the X-Ray Diffraction experiment is shown in (a) of Fig. 1.8 on p. 22. Application of the Bragg Law to a superlattice structure allows the derivation of the following equation:

$$\frac{2\sin\theta_m}{\lambda} = \frac{1}{\bar{d}} + \frac{m}{L} \tag{1.3}$$

where in Eq. (1.3) the mth order reflection occurs at the angle θ_m, λ is the wavelength of the incident X-Rays, $\bar{d}$ is the average spacing between the Bragg planes, and L is the period of the superlattice. By plotting the quantity $(2\sin\theta_m)/\lambda$ versus the superlattice peak index, m, a straight line is attained. Refer to (b) of Fig. 1.8 on p. 22 to see such a plot. From the slope and intercept of the fitted line, the period of the superlattice, L, and the average Bragg plane separation, $\bar{d}$, are attained. Assuming that all of the nitrogen that is present in a period of the superlattice is contained within the single GaN_yAs_{1-y} monolayer, then the monolayer equivalent composition of nitrogen, y, may be written as

$$y = \frac{L}{\bar{d}} \times \bar{y} \tag{1.4}$$

where in Eq. (1.4) $\bar{y}$ is the average nitrogen composition for a period of the superlattice. The above equation essential follows from the definition of $\bar{y}$. By using the average strain, $\bar{\epsilon}$, and the GaAs monolayer thickness, $a_0^{GaAs}/2$, this may be written
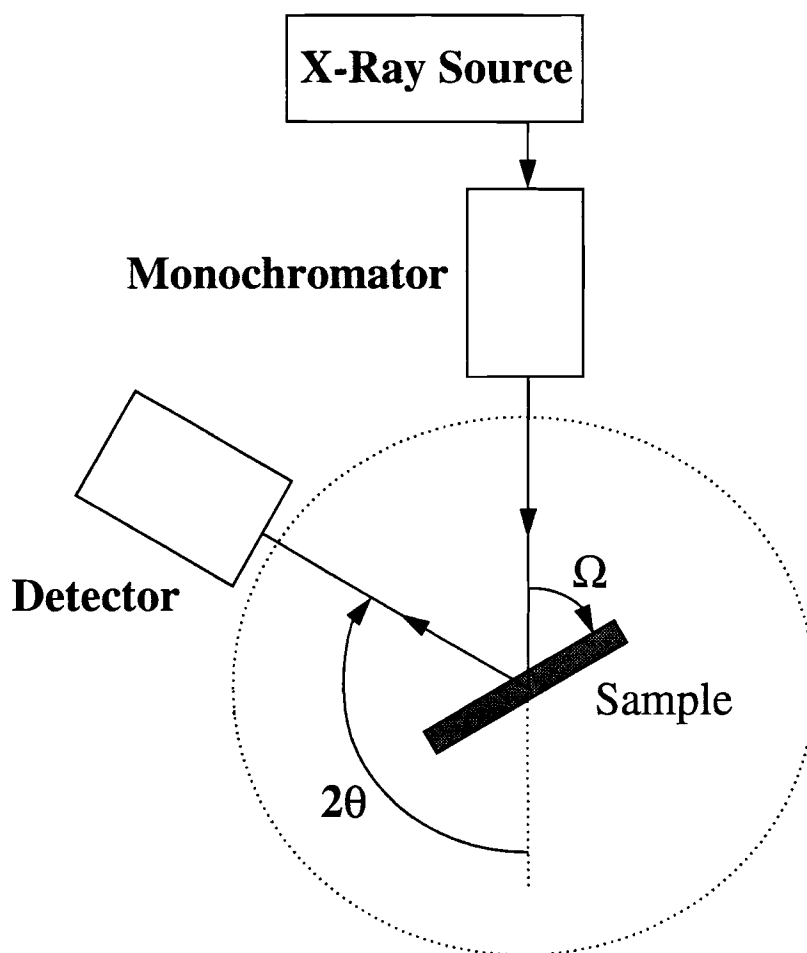
Figure 1.7. Schematic representation of the X-Ray Diffraction experiments conducted.
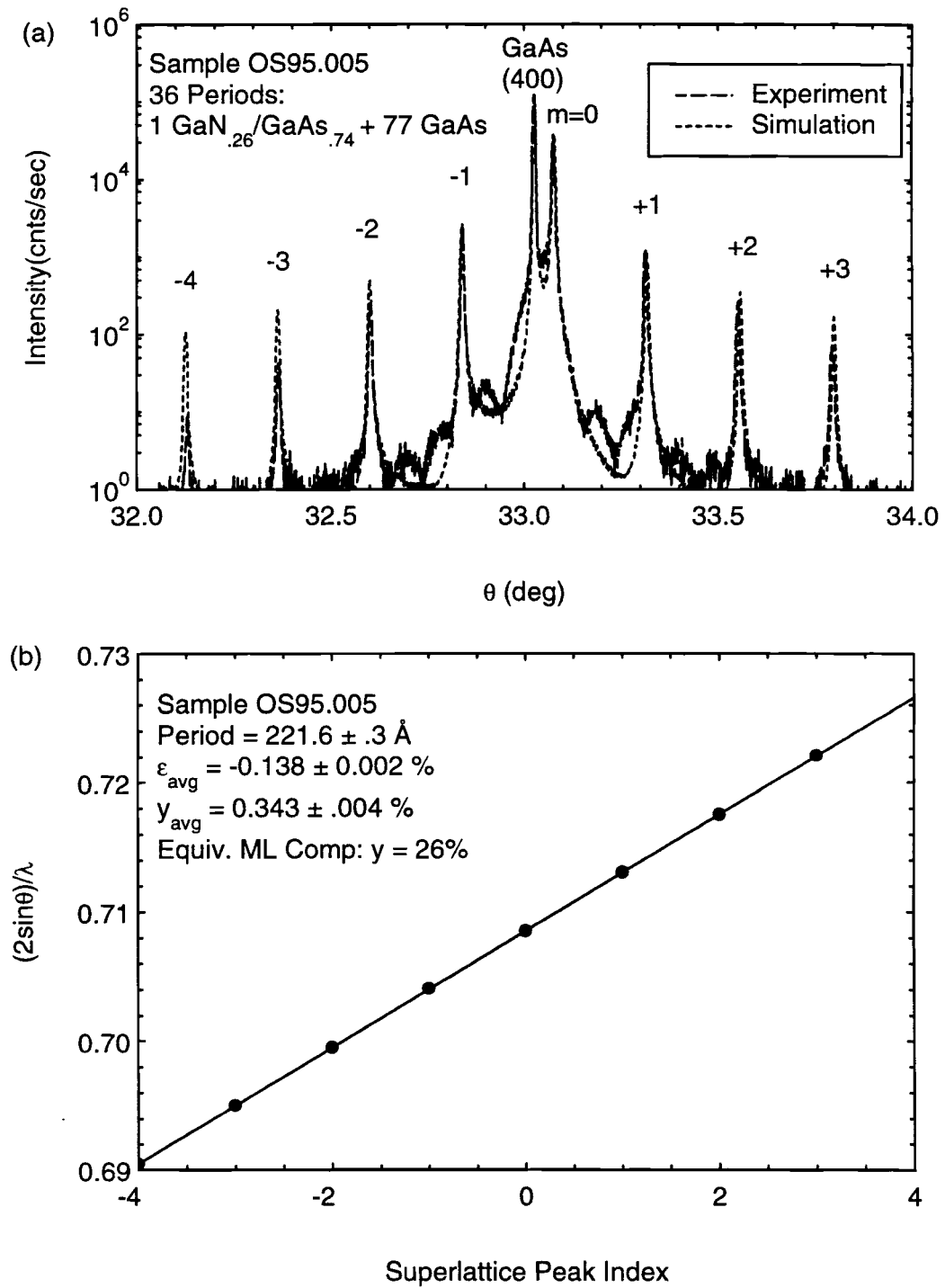
Figure 1.8. The figure above shows (a) typical X-Ray Diffraction data and (b) a plot of $(2\sin\theta_m)/\lambda$ vs. m. The second plot is useful in processing the X-Ray data.

again as:

$$y = \frac{L}{\frac{a_0^{\text{GaAs}}}{4}(1 + \bar{\epsilon})} \times \bar{y} \quad .$$
(1.5)

To attain the Eq. (1.5), the average strain has been taken as:

$$\bar{\epsilon} = \frac{\bar{d} - d_{\text{GaAs}}}{d_{\text{GaAs}}}$$
(1.6)

where d_{GaAs} is the spacing between adjacent Bragg planes in GaAs. Since in this experiment, reflections about the GaAs (400) are observed, $d_{\text{GaAs}} = a_0^{\text{GaAs}}/4$. Furthermore, $\bar{y}$ may be calculated according to the relationship:

$$\bar{\epsilon}(\bar{y}) \approx (1 + \epsilon_T(y))f_0\bar{y}$$
(1.7)

where in Eq. (1.7) ϵ_T is the average tetragonal distortion for the monolayer of the $\text{GaN}_y\text{As}_{1-y}$ alloy and f_0 is the lattice mismatch defined by:

$$f_0 \equiv \frac{a_0^{\text{GaN}} - a_0^{\text{GaAs}}}{a_0^{\text{GaAs}}}$$
(1.8)

with a_0^{GaN} in Eq. (1.8) being the lattice parameter of zincblende GaN. The tetragonal distortion of the alloy layer, ϵ_T, may be estimated by:

$$\epsilon_T(y) = y\epsilon_{\text{GaN}} + (1 - y)\epsilon_{\text{GaAs}}$$
(1.9)

where in Eq. (1.9) ϵ_{GaN} and ϵ_{GaAs} are the tetragonal distortions of GaN and GaAs, respectively. Upon inserting the above equation into the expression for y, it is found that:

$$y = \frac{L\bar{\epsilon}}{\frac{a_0^{\text{GaAs}}}{4}f_0(1 + \bar{\epsilon})(1 + \epsilon_T(y))} \quad .$$
(1.10)

Notice that this expression for y still contains a dependence on y. While an analytic solution is likely possible, solving the problem further quickly becomes intractable. It is easiest by far, to solve the above equation for y numerically. A simple program can be written in almost any programming language to accomplish this task. In this particular case, a spreadsheet was used for the calculation.

1.4   SPECIFIC CONTRIBUTIONS OF THIS THESIS

A number of significant accomplishments will be presented in this thesis. For the work represented in Chapter 2, a number of growth runs aimed at growing bulk GaN epitaxial films on GaAs (100) substrates were conducted. From the work that will be presented there, it will be shown first that GaN could be grown on GaAs (100) substrates; a monumental accomplishment considering the large lattice mismatch of the two materials. Furthermore, a preliminary assessment of the most pertinent growth parameters is performed. Also, the effects of variations in these parameters on the quality of the resultant films is studied. In this study, a number of RHEED images for various surface conditions will be reported; one of which, the (3×3) surface reconstruction pattern, had not previously been reported. Finally, in the growth of the samples for this study, a distinct mode by which the growth of GaN is self-limited is observed.

The previously unreported (3×3) surface reconstruction pattern was of great enough interest to warrant further study. Also, the need to understand the mode of self-limited growth observed in the growth of bulk GaN suggested that a fundamental study of the interaction of the nitrogen plasma with the GaAs substrates needed to be conducted. In this study, which will be presented in Chapter 3, two distinct sets of experiments were conducted. From the first set of experiments, it will be shown that a brief exposure of a GaAs surface to the nitrogen plasma results in a GaN monolayer on the sample surface that is manifestly more stable than GaAs surfaces under similar conditions. This will also demonstrate that a nitrogen–for–arsenic anion exchange process is occuring. Despite this comparative stability, it will be shown that the nitrided monolayer does exhibit a slow temperature dependent decay, the outcome of which is affected by the presence or absence of the As flux onto the sample. Further evidence will indicate that this nitrided surface can be commensurately overgrown with GaAs. During this overgrowth, it will be noted that surface segregation of nitrogen during the GaAs overgrowth is occuring. Finally, it will be shown that longer periods of exposure result in a

rough, strain-relaxed GaN surface that can not be overgrown with commensurate GaAs.

The results of the first group of experiments suggested a second set of experiments in which $GaN_yAs_{1-y}/GaAs$ superlattices were grown to study the strong temperature dependence of the nitrogen re-evaporation and segregation kinetics. The results of this study will demonstrate that the superlattices can be grown. Also, from studies of these superlattices, it will be shown that there exist two distinct growth regimes which determine the amount of the nitrogen incorporated into the $GaN_yAs_{1-y}/GaAs$ superlattices. Finally, the results of the studies of the kinetics make very strong suggestions as to the adjustments necessary to the growth parameters for improvements in the growth of epitaxial GaN films on GaAs substrates.

CHAPTER 2

GROWTH OF EPITAXIAL ZINC BLENDE GaN
FILMS ON GaAs (100) SUBSTRATES

2.1 INTRODUCTION

A great deal of information is available via literature searches concerning the material properties of GaN. Comparatively little information is available concerning the growth of zincblende GaN by Plasma-Assisted Molecular Beam Epitaxy. Despite the information that is available, the parameters of the growth are dependent on the exact geometry of the particular MBE system in which samples are grown. Presented in this chapter will be a discussion of the preliminary experiments conducted in the growth of epitaxial zincblende GaN films on GaAs (100) substrates. In particular, the exact parameters of a set of experimental growth runs, labeled OS94.004 through OS94.012, will be discussed as well as the rationale for the adjustments made for each successive growth experiment. In several of the samples, a mechanism of self-limited growth is observed. The first attempts to more fully understand this mechanism and to interactively develop a solution will be handled in Chapter 3.

2.2 EXPERIMENTAL

Each of the samples in this series were grown on heavily Silicon-doped GaAs (100) substrates. Each substrate was prepared *in situ* before the deposition of GaN epitaxial layers. These GaAs substrates were prepared by the following well-established and accepted procedures. Each substrate was first heated under ultra-high vacuum conditions until the surface oxides begin to vigorously desorb. This desorption is known to occur at 580 °C. After this desorption, RHEED images yield

a spotty (2×4) surface reconstruction pattern. This pattern will usually have spots rather than the normal streaks because the substrate surface is microscopically very rough. The (2×4) surface reconstruction indicates an As-stabilized GaAs surface.

After the desorption of surface oxides, a 1 μm GaAs buffer layer is deposited. In each case, the growth rate is nominally set for 1.00 ML/sec or $\approx$ 1.02 μm/hr. The As cell is set to generate approximately a 3-to-1 overpressure of As_2 to Ga. The temperature setting for the Ga cell is initially determined from previous calibration data recorded by studying RHEED oscillations. Initially, the substrate temperature is set to 580°C and is raised after a few minutes of growth to approximately 600°C. The growth of the buffer layer is periodically interrupted so that RHEED oscillation data may be recorded during each growth run. In doing this, a direct measurement is made of the growth rate. This provides greater accuracy and control over the thickness of the deposited films. In each case, the RHEED patterns observed during the growth of the buffer layer evolve during the first few hundred angstroms of growth from the spotty pattern observed after the desorption of the surface oxides to a streaked pattern. This indicates a smoother sample surface. A representative set of photographs showing the (2×4) surface reconstruction pattern are given in Fig. 2.1 on p. 28.

Upon completion of the buffer layer, zincblende GaN films were deposited on the prepared GaAs surfaces. The most important parameters in the growth of the GaN films have proven to be substrate temperature, the Ga flux or arrival rate, and the nitrogen plasma condition. In this context, both the power of the microwaves incident upon the plasma cup and the nitrogen flow rate are involved in the nitrogen plasma condition. In each of the growth runs in this sample set, the nitrogen flow rate during the GaN growth is fixed at the same condition throughout—specifically 26 sccm.* The instrument used to generate the microwaves for the ECR plasma allows control of the forward or applied power of microwaves to the plasma cup. Also, this instrument measures the power of reflected microwaves from the plasma

---

*This flow rate suffers from an intrinsic error since the flowmeter used is calibrated for air rather than pure nitrogen. Though an absolute measurement is not available with the current equipment, this flow rate is highly repeatable.
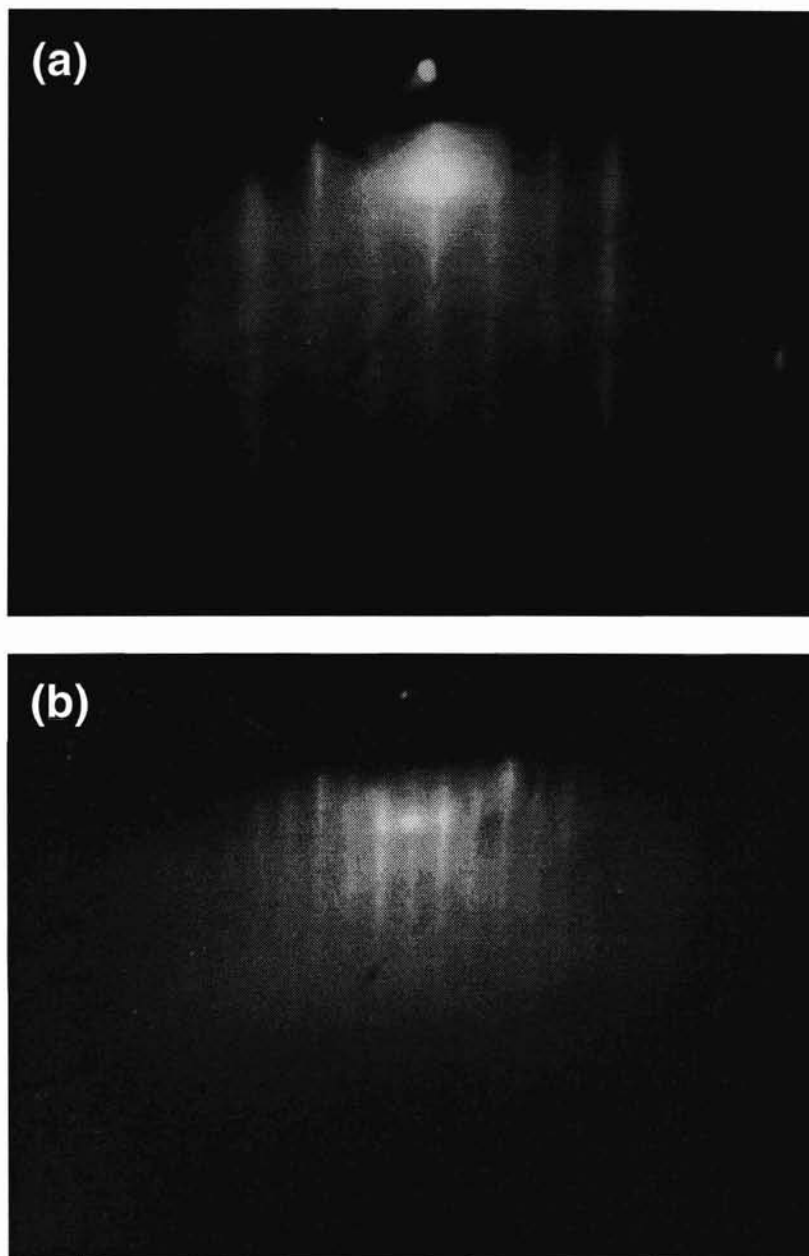
Figure 2.1. Shown in the figure are typical images observed of a (2×4) surface reconstruction pattern observed for GaAs. In the figure above (a) is along the [110] direction and (b) is along the [1$\bar{1}$0] direction.

cup. The physically relevant variable in the growth is most likely the difference in the two power levels. However, to within experimental repeatability, the reflected microwave power was approximately 32 W for each growth run. Therefore, as a matter of convenience in referring to the growth conditions, the forward power of microwaves will be used for reference.

The initial stages of the growth of GaN on the GaAs surfaces are the most critical. In each growth experiment, the same basic sequence of events was followed to initiate the growth. The steps in this sequence are as follows. Prior to the initiation of growth, a controlled leak of N_2 gas was established through the ECR source while a continuous flux of As_2 was provided to maintain the As-stabilized surface. For each growth run, the sample was initially set to a temperature of 580°C and the Ga cell was set to provide a flux rate that would provide 0.05 ML/sec of growth under GaAs growth conditions. With the growth chamber in this state, each of the following events were manually actuated in rapid sequence. First, the microwave power supply was turned on and the ignition of the plasma was verified. Next, the shutter covering the nitrogen source was opened. Lastly, the As shutter was closed simultaneous to the opening of the Ga shutter. This sequence of steps was typically carried out in approximately two to five seconds. As a matter of convention, growth was conducted for approximately 45 minutes at this condition, then the sample temperature was ramped in a consistent manner to approximately 620°C. In successive runs, the Ga arrival rate and the forward microwave power were adjusted to optimize the growth. At this same time, adjustments were made, as necessary, to the microwave power supply and the Ga cell to establish the growth parameters chosen for each particular growth run. Table 2.1 on p. 30 shows the chronological evolution of the growth parameters.

2.3   RESULTS AND DISCUSSION

The chronological evolution of the various parameters in Table 2.1 suggests that significant feedback was taken from each of the growth runs and used to modify

Run Number	Sample Temperature (°C)	Ga Cell Temperature (°C)	Microwave Power (watts)
OS94.004	620	907	75
OS94.005	620	960	75
OS94.006	620	907	80
OS94.007	620	907	100
OS94.008	620	938	100
OS94.009	620	960	100
OS94.010	620	960	150
OS94.011	620	938	100
OS94.012	633	907	100

TABLE 2.1. Chronological evolution of the GaN growth parameters.

the parameters of the subsequent growth runs. In this section, the observations made of each growth will be briefly presented and discussed.

2.3.1 OS94.004

Sample OS94.004 was an attempt to grow a thin film of epitaxial zincblende GaN on a GaAs substrate. As shown in Table 2.1 the parameters chosen for this sample were a substrate temperature of 620 °C, a forward power of 75 W, and a Ga cell temperature sufficient to provide a Ga arrival rate of 0.05 ML/sec under GaAs growth conditions. The forward microwave power of 75 W was chosen as it appeared to be the minimum power that would sustain the nitrogen plasma.

The outcome of this growth run was quite fortuitous considering it was the first attempt at growing a GaN sample by this method. Successfully grown was a GaN film initially believed to be approximately 1500 Å in thickness. Also, there where some very interesting images provided by RHEED. For simplicity in this growth run, only RHEED patterns in the [110] direction were monitored throughout the growth. An evolution of the RHEED patterns was noted even in the Polaroid photographs taken of the RHEED images. The characteristic GaAs 2× surface reconstruction for the [110] direction was observed to evolve immediately into a 3× surface reconstruction pattern. Then, with progressive deposition, this evolved to a 2× surface reconstruction with greater separation of the diffraction lines. This 2× pattern was initially very spotty and eventually grew into streaks. The spotty pattern indicates that the surface is rough or faceted. RHEED patterns composed of streaks indicate that the surface is smooth. As the RHEED patterns image the surface in reciprocal space, the greater separation of the diffraction lines is consistent with imaging a GaN surface; note that GaN has a smaller lattice parameter than does GaAs. Recorded RHEED images of this evolution are presented in Fig. 2.2 on p. 32.

Intermixed with the GaN 2× reconstruction image were lines normally observed in the GaAs RHEED image; in particular, the $\pm\frac{1}{2}$ order lines were present. These lines were persistent for approximately 30 minutes. It should be noted that

(a) Before GaN growth.

(b) A few seconds of GaN.
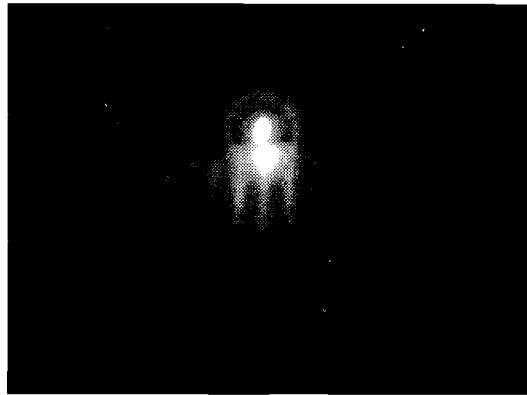
(c) 4 minutes of GaN.

(d) 3 hours of GaN.
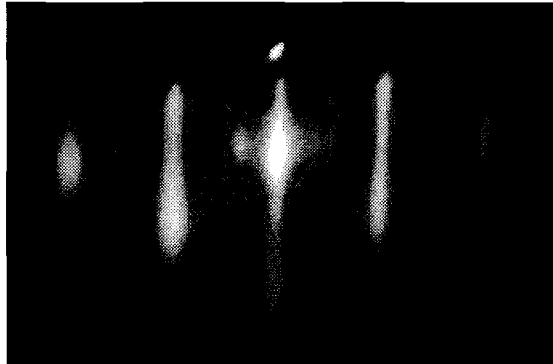
Figure 2.2. RHEED images observed during the characteristic evolution of the surface immediately following the onset of growth of GaN on GaAs. Shown above are the images along the [110] azimuth at the times indicated. Images above show (a) the GaAs $2\times$, (b) the transient $3\times$, (c) the spotty GaN $2\times$, and (d) the streaked GaN $2\times$ pattern.

in this time, approximately 45 monolayers of GaN should have been deposited. Considering that the electron beam should only penetrate a few monolayers into sample surface,[5] clearly these lines should not have been observed. As the acquisition of more experimental data will aid in the interpretation and explanation of this observation, potential explanations for this phenomenon will be deferred until Chapter 3. As a final note on the growth details, a final RHEED pattern was attained having a (2 × 2) surface reconstruction. The RHEED images presented in Fig. 2.3 on p. 34 show this (2 × 2) surface reconstruction pattern. This run demonstrated that the set of parameters used were suitable though not necessarily optimal.

Ex situ inspection of the sample showed that the surface was hazy due to non-optimal growth conditions. Also, differing degrees of haziness and variations in the apparent color, due to thin film interference, indicated that a temperature gradient existed across the plane of growth. Non-uniform heating of the sample is unfortunately an artifact of samples that are improperly mounted by Indium soldering. Inspection of the residual Indium on the back surface of the sample showed that non-uniform wetting had occured.

2.3.2   OS94.005

For sample OS94.005, an effort was made to increase the growth rate of GaN. With all other growth conditions being equal to those of the previous sample, the Ga cell temperature was set to 960°C. Under GaAs growth conditions, this would provide a growth rate of 0.15 ML/sec.

In the growth of the GaN film, the same initial evolution of the RHEED images observed in the growth of sample OS94.004 were noted. Again, this evolution of images as viewed along the [110] direction was from the streaky GaAs 2× pattern to a streaky 3× pattern, to a spotty 2× pattern with greater separation between the diffraction orders, and finally to a streaky 2× pattern with the larger separation of the diffracted lines. However, in this sample, the $\pm\frac{1}{2}$ order diffraction lines from the GaAs pattern were not observed. Also, despite being grown
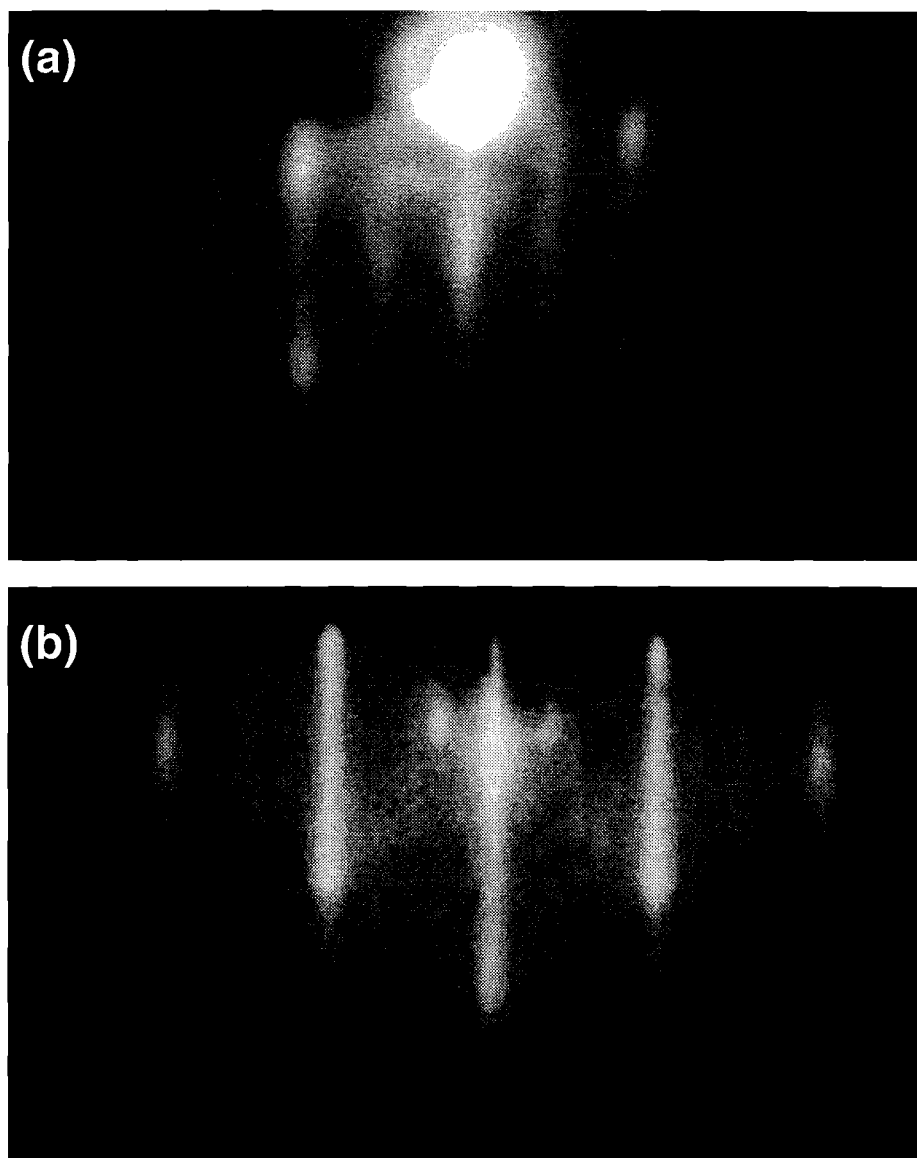
Figure 2.3. Presented in the RHEED images above are the diffraction patterns for the GaN film grown as sample OS94.004 along (a) the [110] and (b) the [1$\bar{1}$0] directions. The images shown were taken with the sample at 620°C, after 6.7 hours of growth, or with an estimated 1500 Å of GaN. The surface is exhibiting a (2 × 2) reconstruction.

on a buffer layer of very high quality, the RHEED images never became sharply resolved and were quite spotty throughout. This indicates that the sample surface was not microscopically smooth and that the film quality was poor. Also, of greater importance, after approximately 1.5 hours of deposition at the higher growth rate, the substrate temperature as read by the MBE system's optical pyrometer began to drop, despite the fact that the power level of the sample heater was increased to compensate. Simultaneous to this, there was an extreme decrease in the intensity of the RHEED images. At this point, it was obvious that the sample surface had deteriorated beyond possible recovery, and the growth run was terminated.

Hence, at these particular growth conditions, it was observed that epitaxial growth was self-limited. From the RHEED images, it appeared that the sample surface had become coated with Ga. Possible explanations for this could be any of the following: (1) the plasma had extinguished due to an excessively low microwave power level, leaving no active species of nitrogen to react at the surface; (2) the flux of Ga was simply too large when compared to that of the species of nitrogen responsible for growth; (3) the emissivity of the GaN film was lower than that of the GaAs film for which the optical pyrometer was calibrated. Therefore, the film would have been emitting less of the IR radiation which the optical pyrometer detects, causing the lower temperature reading. In reality, the temperature of the sample would have been increasing as it was emitting energy less efficiently. Furthermore, this effect of the increasing temperature was exaggerated as the growers responded by increasing the power level of the sample heater. As at least two other indicators showed that the plasma had not extinguished, (1) above is quite unlikely. Also, since there was no problem of this type in the previous growth run which was identical except for the Ga flux rate, (3) above is also unlikely. Hence, it appears that the Ga flux was simply too great for the particular plasma condition used in this experiment.

2.3.3   OS94.006

It was decided that the most logical direction to proceed after run OS94.005 was to determine a nitrogen plasma condition that was more conducive to the growth of GaN before trying to optimize the other growth parameters. There were two important considerations for this decision. First, as it appeared that there was an insufficient quantity of the nitrogen species responsible for growth in the deposition of the GaN epitaxial film for sample OS94.005, it seemed logical to move to a higher plasma power. Second, moving to a lower plasma power presented serious logistical difficulties in terms of generating a stable nitrogen plasma. As the growth of sample OS94.004 did not appear to be self-limited, nearly identical growth conditions were chosen for sample OS94.006. For the growth of this sample, the forward plasma power was increased from 75 W to 80 W.

In the growth of OS94.006, again, much the same initial evolution of RHEED images was observed. In this case, the $\pm\frac{1}{2}$ order diffraction lines from the GaAs RHEED pattern along the [110] direction were persistent throughout the sample growth. Also, following the evolution of RHEED patterns, there was a $2\times$ reconstruction pattern in the [110] direction throughout the growth. Furthermore, after approximately 6.5 hrs of growth, it was noted that the sample had a streaky (2×4) surface reconstruction. The RHEED images showing this surface reconstruction are presented in Fig. 2.4 on p. 37.

At the end of the sample growth, the RHEED images began to show polycrystalline features. Therefore the run was terminated after approximately 2000 Å of GaN growth. The polycrystalline features observed in the RHEED pattern can most easily be explained as being caused by a cold region on the sample. Again, a cold region could be caused by poor Indium wetting of the back surface of the sample.
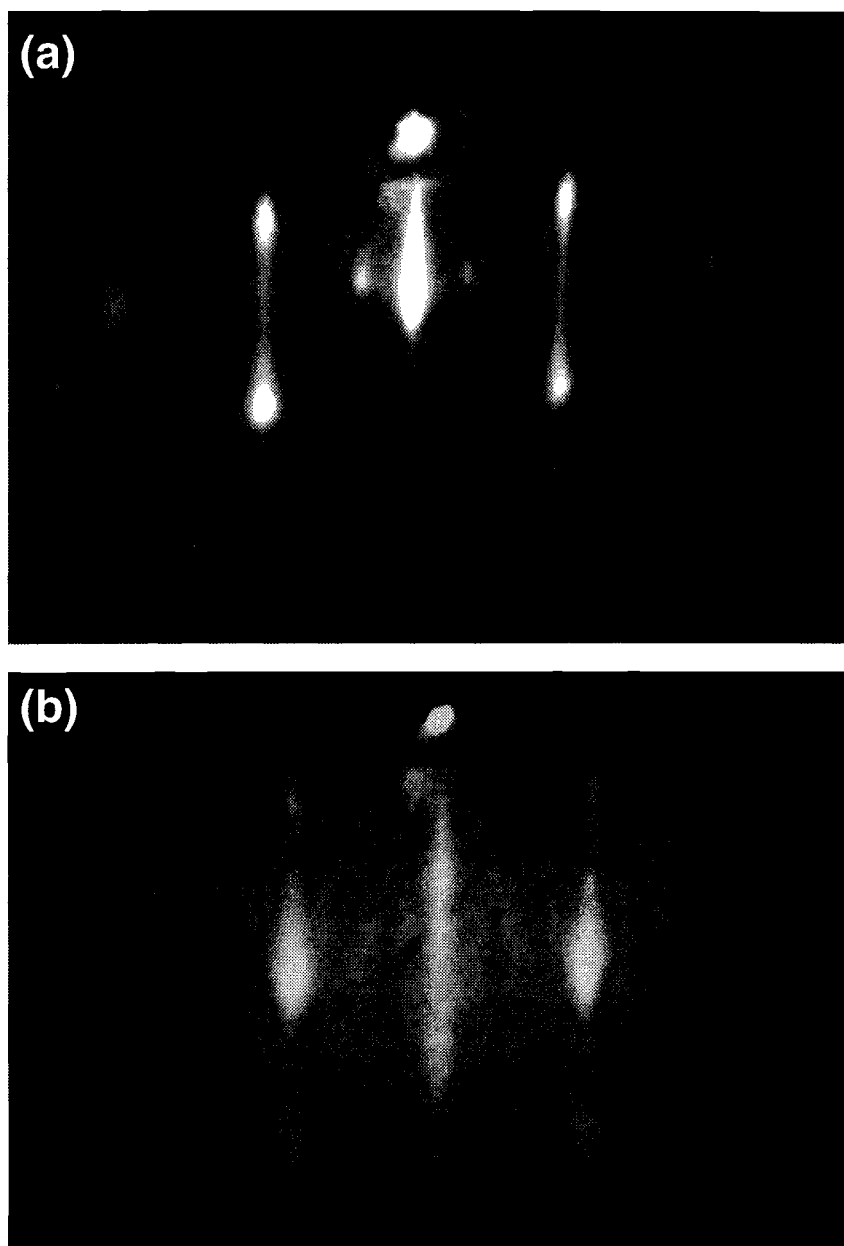
Figure 2.4.   The RHEED images above show the (2 × 4) surface reconstruction of a GaN surface observed during run OS94.006. Images (a) and (b) are taken along the [110] and [1$\bar{1}$0] direction, respectively. The photos above were taken with the sample at 625°C, after 6.5 hours of deposition or an estimated 1600 Å of GaN.

2.3.4   OS94.007

Having experienced what looked like a success in the previous run, the decision was made to move to still a higher plasma power to see if the even better growth results could be attained. In the growth of OS94.007, the forward microwave power was set to 100 W and all other growth parameters and procedures were kept the same.

For the sample grown here, it first should be noted that the GaAs buffer layer was not as high a quality as those grown for previous runs. In this sample, the initial evolution of the RHEED images is difficult to comment upon accurately because the images were initially of only mediocre quality. Fortunately, this surface did evolve into what was apparently a high quality GaN sample. While some time was required to grow out of the the mediocre onset due to the buffer layer, very sharp and streaky RHEED patterns were attained in all directions. In particular, the sample exhibited a (2×2) surface reconstruction in the early stages of the sample growth. It can be seen from the RHEED image photographs that the surface reconstruction changed from a (2×2) to a (2×4) surface reconstruction between 3.3 and 4.5 hours of growth. The growth was terminated by choice after the deposition of approximately 2300 to 2400 Å of GaN. The final surface exhibited a nicely resolved (2×4) surface reconstruction. It is worth pointing out that the same (2×4) surface reconstruction was observed the next day *at room temperature.*

Postgrowth inspection of the sample using an ordinary stereo-microscope indicted that the surface was uniform but rough. Furthermore, there was a slight fluctuation in the apparent color of the surface from green to a greenish-yellow. This indicates that there was a small thermal gradient across the sample surface during growth. However, despite this difficulty and the poor starting surface, this set of growth conditions yielded the the highest quality sample to that point in time.

2.3.5   OS94.008

Having attained reasonable success in the growth of sample OS94.007, the next step was to try the same set of growth conditions with a higher growth rate. Sample OS94.008 was grown at the same sample temperature and nitrogen plasma condition as sample OS94.007. Recall that these were a substrate temperature of initially 580°C which is later ramped to 620°C, and a forward microwave power of 100 W to generate the nitrogen plasma. However, in this particular growth, the Ga cell was set to an operating temperature of 938°C, which translates ideally to a growth rate of 0.10 ML/sec under GaAs growth conditions.

It is assumed that the same evolution of the RHEED images occured during the initial stages of the GaN growth for sample OS94.008. In the onset of this sample growth, the RHEED images were fuzzy, and it was difficult to accurately resolve the finer details of the RHEED images. The RHEED photos taken at 2 hours of growth show the first well resolved RHEED images. This indicates that the sample surface was initially rough and grew into a smoother more planar surface. Images of the [110] direction RHEED patterns show the characteristic GaN 2× surface reconstruction along with the $\pm\frac{1}{2}$ order lines of GaAs. These lines persisted in the growth for approximately 6 hours. Also, by surveying the [1$\bar{1}$0] direction as well, it can seen that the surface in this state is exhibiting a (2 × 4) surface reconstruction. The RHEED patterns continued to become quite sharp as the growth continued. At the conclusion of the GaN growth, a clear (2 × 4) surface reconstruction could be seen.

These results seem to indicate that under the current set of conditions, substrate temperature of 620 °C, Ga flux rate of 0.10 ML/sec, and a microwave forward power setting of 100 W, are conducive to the growth of high quality epitaxial zincblende GaN films. *Ex situ* inspection of the sample indicates that the sample quality is commensurate with the other growth runs to this point; however, the sample surface exhibited some imperfections. Due to non-uniform heating of the substrate, the color of the sample surface, due to thin film interference, varied from

violet to blue-violet. Also, the sample appears mirror-like and smooth in normal viewing; yet when examined under a stereo-microscope, a uniform surface roughness can be observed. Finally, when viewing the surface via glancing incidence light, it could be seen that the surface was uniformly hazy.

2.3.6   OS94.009

Having attained success through the adjustments made for the growth of sample OS94.008, sample OS94.009 was an attempt to improve the growth rate even further. In this growth run, the Ga arrival rate was set to 0.15 ML/sec under GaAs growth conditions by setting the Ga cell temperature to 960°C.

The GaAs buffer layer that was grown was comparable in quality to those of the other samples. Initially, the GaN film was grown at a rate of 0.05 ML/sec for approximately 1 hour rather than the normal 45 minutes. At this point, the Ga cell temperature was ramped up to a condition appropriate to provide the targeted flux rate of 0.15 ML/sec under GaAs growth conditions. The RHEED images throughout this growth run were a bit fuzzy. With the increased Ga flux rate, the RHEED images appeared not to change for approximately 50 minutes. However, over the next 40 minutes, there was an extreme loss of both RHEED pattern intensity and quality. Furthermore, there was a magnanimous drop in the substrate temperature as measured by the optical pyrometer. This run was terminated soon after these problems were recognized. Clearly, from this description of the symptoms, this sample appears to have been self-limited in its growth by the same mechanism as sample OS94.005.

It is clear from what is described above that an upper bound to the Ga flux that can be used for high quality growth of GaN has been determined for this particular plasma condition. It should be noted that there is no reason to expect that this is the least upper bound for the Ga arrival rate at this nitrogen plasma condition.

2.3.7 OS94.010

The same growth conditions for sample OS94.009 were used for the growth of sample OS94.010 with the exception of the applied plasma power. In this run, a higher plasma power, 150 W, was used in hopes of creating a suitable nitrogen plasma for growth at the higher Ga arrival rate.

The RHEED patterns observed at the end of the buffer layer growth indicted that the buffer layer was of the same uniformly high quality as those grown for previous samples in this study. For this sample, as in each before it, a thin initial layer was grown at conditions established as suitable for growth at a slower rate. Immediately upon initiation of the GaN layer, polycrystalline features were observed. These features seemed to diminish with continued deposition of GaN. After approximately 40 minutes of growth at that condition, the RHEED patterns were observed to be spotty, indicating a rough GaN surface. This was not far different from that which had been observed in previous sample growths. Upon restarting the growth with the plasma power level at 150 W forward power and the Ga flux rate set to 0.15 ML/sec for equivalent GaAs growth condition, the overall intensity of the RHEED patterns immediately dropped. A reasonable set of RHEED patterns were attained by re-optimizing the imaging conditions. At these new conditions, the overall image was still quite dim. The image was composed of diffraction lines that were somewhat streaky but still exhibited a spotty nature. Over the course of the growth of this sample, the intensity and quality of the RHEED images consistently decreased. After 3.33 hours of growth at the elevated power condition, the RHEED images began to exhibit polycrystalline features. At approximately 5 hours of growth at this condition, it was decided to terminate the growth run as the surface had become damaged beyond any reasonable hope of recovery.

A possible explanation for this result is that the effect of high energy ions from the plasma damaged and roughened the surface. This combined with the high

Ga arrival rate could readily cause the effect of RHEED images that become dimmer and lower in quality. Also, the presence of the initial polycrystalline features in the RHEED images suggest that a cold spot may have existed on the sample substrate. Optical pyrometer readings early in the growth experiment suggested that the temperature of the sample was uniform. However, the optical pyrometer may be positioned so that it always measures the temperature at the center of the sample. Therefore, it is possible that the early indications from the optical pyrometer were misleading depending on the positioning of the optical pyrometer for that particular growth experiment.

Despite the difficulties with the optical pyrometer and the polycrystalline growth, the fact the the RHEED quality immediately dropped at the onset of growth at the elevated plasma power level and increased Ga arrival rate indicates that these particular growth conditions are not suitable for the growth of high quality epitaxial GaN.

2.3.8 OS94.011

Samples OS94.011 and OS94.012 were not grown as the next steps in the study presented to this point. These two samples were actually grown in an effort to produce relatively thick epitaxial films of zincblende GaN for further study. However, there were some observations made in the growth of these two samples which are relevant to the study which is being presented. As the principle interest in the growth of these samples was to produce the samples for further study, not to study the growth, growth conditions were selected that allowed for the fastest possible growth of GaN over the manifold of conditions that had been investigated at that time. To grow relatively thick films, it was necessary to grow for an extended period of time. The lack of personnel capable of working "around the clock" required that the samples be grown for a number of consecutive days. In the case of sample OS94.011, this was for two days, and three days for sample OS94.012.

In the growth of sample OS94.011, a buffer layer of exceptional quality as indicated by RHEED was deposited. The GaN film was initially grown at a substrate temperature of 620°C, a microwave power of 100 W, and a Ga arrival rate of 0.05 ML/sec for equivalent GaAs conditions. After approximately 1 hour of growth, the Ga cell temperature was ramped up to provide a Ga arrival rate of 0.10 ML/sec under GaAs conditions. The sample was grown at this condition for 4 hours. At that time, a decrease in the RHEED image intensity was observed and in response, the Ga arrival rate was reduced to the 0.05 ML/sec level. After an additional 2.5 hours of growth, the deposition was stopped for the day. The sample was left at a substrate temperature of 400°C under ultra high vacuum conditions.

Growth of sample OS94.011 was resumed the next morning. One of the oddities of this growth run was that the next morning, the RHEED images appeared much sharper than the night before, even before deposition started. It is expected that the surface would improve slightly due to the thermodynamic arguments given in Chapter 1. However, it was puzzling to see this scale of improvement in the surface since the substrate temperature was only 400°C and surface mobility should have been quite low.

In the second day of growth, several attempts were made to raise the Ga cell temperature incrementally. It was expected that growth was possible at a Ga arrival rate of 0.10 ML/sec because of the results of run OS94.008. However, each attempt at raising the Ga cell temperature resulted in the loss of RHEED intensity after a short period of time. In each case, lowering the Ga cell temperature back to the 0.05 ML/sec level appeared to result in an return of the RHEED screen intensity with only a slight net degradation of the sample. The total deposition was estimated to be approximately 4020 Å.

The RHEED images were streaky with a slightly spotty nature during the first day and part of the second day, but became quite spotty later in the second day. In particular the images along the [110] direction were distinctly more streaky than those along the $[1\bar{1}0]$ direction. RHEED images showed (2×4) surface reconstructions for the first day and part of the second. In the later portion of the second

day, the poor quality of the RHEED images made exact determination of the surface reconstruction difficult. The persistent GaAs lines were observed throughout the first day in the usual fashion. However, the GaAs lines could not be observed in the second day of deposition.

The results of this sample growth suggest that the growth conditions established by sample OS94.008 are not suitable for extended depositions. This suggests that there is possibly another variable in the growth process that has not been well controlled or one that is not being controlled well enough.

2.3.9   OS94.012

Sample OS94.012 was grown at nearly the same conditions as sample OS94.011. The particular differences in this growth were the following. (1) There were no experiments conducted with the Ga arrival rate. The Ga arrival rate was set for 0.05 ML/sec and was not adjusted again. (2) The sample was grown at a slightly higher temperature, approximately 635 °C. At the time, it was believed that fuzzy RHEED patterns were caused by insufficient surface mobility forcing the surface to be rough. Therefore, the substrate temperature was increased slightly to allow for a smoother growth surface.

The GaAs buffer layer that was grown for this sample was again of exceptional quality. The RHEED images show many details that cannot be seen on poorer surfaces. The RHEED images for the GaN growth showed the same basic evolution as in previous growth runs except that the streaky (2×4) GaN images were attained more quickly and the persistent GaAs diffraction lines dissipated more quickly than in previous runs. RHEED images that were streaky but showing a slightly spotty nature were observed for the remainder of the 8.75 hrs of growth on the first day.

Again, the sample was left at 400°C overnight. However, the next day, the RHEED images were slightly poorer than the evening before. Because there were only slight differences though, this could be explained as imaging artifacts. The growth for the first 7 hours was uneventful and RHEED images remained sharp. At approximately 7 hours of growth, the intensity of the RHEED images began

to decrease. To compensate for this, the substrate temperature was gradually increased in small increments over several hours. At 15.5 hours of growth, it was noticed that the substrate temperature as recorded by the optical pyrometer had dropped from 644°C to 633°C. Then at 15.75 hours of growth, the optical temperature readings had dropped from 633°C to 463°C with no further change to the substrate heater power level. Furthermore, an enormous drop in RHEED image intensity and quality was observed. Efforts were made for almost 9 hours, with little success, to improve the quality of growth by reducing the Ga arrival rate, making careful adjustments of the nitrogen partial pressure, and adjusting the substrate temperature to improve RHEED images.

The possible cause(s) for the loss of the surface quality include the following. (1) The higher substrate temperature decreased the efficiency with which the nitrogen was permanently incorporated into the surface. (2) An observed drop in the nitrogen pressure level due to a fluctuation may have caused the nitrogen plasma to extinguish, causing the GaN surface to be coated with Ga. Alternatively, the fluctuation may have significantly reduced the production of the excited or ionized nitrogen species responsible for growth, again resulting in a Ga coating of the surface.

2.4 CONCLUSIONS

A number of growth runs were conducted for the purpose of determining suitable growth conditions for the growth of GaN epitaxial films on GaAs (100) substrates. In these experiments, each sample growth incorporated successive adjustment to the conditions of the previous growth experiments. The successive adjustments were small "tweaks" to two of the most important growth parameters: the microwave plasma conditions and the Ga arrival rate. Since two parameters were already under study, no attempt was made in these experiments to rigorously understand the effect of the substrate temperature on the growth.

The results of these experiments suggest a particular growth condition to use for the growth of epitaxial thin films of zincblende GaN on GaAs (100) substrates.

By attempting to grow these films, the implication was made that if the substrate temperature and plasma condition are accurately maintained at the conditions established in these experiments, then high quality epitaxial films can be grown at a growth rate of 0.05 ML/sec. The growth of such a sample should not be self-limited so long as the growth conditions are rigorously and accurately maintained.

In the growth of these samples above, several different RHEED images representing different surface reconstructions were observed for apparently very similar conditions. In particular for GaN growth, a (2×2), a (2×4), and a (3×3) were observed. In the case of GaAs growth, a "phase diagram" of sorts has been developed for associating a particular surface reconstruction with a particular growth condition.[5] It would be of great interest and usefulness to develop such a "phase diagram" for the growth of GaN. For this to be possible, it will be necessary to fully understand the nature of the various RHEED patterns which are associated with a particular surface reconstruction, and the conditions under which they occur.

Also, in this study, a distinct mechanism by which the growth of GaN is self-limited was observed. Namely, this self-limiting mechanism was due to excess Ga on the surface of the sample inhibiting the epitaxial growth. Currently, the most probable cause for this excess Ga at the surface is a Ga arrival rate that is simply too large as compared to the that of the species of nitrogen that is responsible for growth.

CHAPTER 3

NITRIDATION OF GaAs SURFACES UNDER
NITROGEN PLASMA EXPOSURE
3.1 INTRODUCTION

In the previous chapter, an extensive exercise was undertaken to determine
optimal conditions for the growth of zincblende GaN on GaAs (100) substrates.
Several difficulties were encountered; in particular, there was a common mode of
self-limited GaN growth. Specifically, this mode was an insufficient supply of the
appropriate nitrogen species as compared to that of the Ga arrival rate. Further-
more, several different RHEED images where observed for only slightly dissimilar
growth conditions.

In this chapter, an attempt will be made to understand one the most interest-
ing of the RHEED images observed in the previous chapter. This RHEED pattern
was that of the (3 × 3) surface reconstruction. This RHEED pattern was observed
as a transient state between the (2 × 4) surface reconstruction of GaAs before the
onset of GaN growth and the (2 × 2) pattern which is observed early in the growth
of the GaN films. It is the transient behavior at the initiation of growth that makes
the (3 × 3) more interesting, at this point, than the other observed reconstruction
patterns. The quality of the initial surface upon which epitaxial layers are depos-
ited greatly affects the quality of the film that is grown. Given this, the (3 × 3)
surface reconstruction is of interest because the epilayers that are deposited at the
time in which the (3 × 3) surface reconstruction is observed are more crucial to the
overall quality of the film that is grown. Also, it is obvious from the observed mode
of self-limited growth of GaN from the previous chapter that simply not enough
is known about the nature of the nitrogen plasma and how it affects the growth of
epitaxial films and how it affects the epilayers that have already been deposited.

For the work presented in this chapter, two distinct but related sets of experiments were performed in hopes of learning how the nitrogen plasma affects growth. In performing these experiments, the ambition was to learn more about the nature of the nitrogen plasma and how it affects the growth of samples, and being able to use this acquired knowledge to suggest improvements in the conditions for the growth of zincblende GaN.

3.2 EXPERIMENTAL

As already mentioned, there were two distinct sets of experiments performed in the research composing this chapter. Each of these sets of experiments required minor external modifications be made to the MBE system. For the first set of experiments, it was necessary to modify the RHEED imaging system. The modification made was the mounting of a CCD camera to the external chamber wall, allowing the RHEED patterns to be imaged by the CCD camera. Images were recorded using a S-VHS video cassette recorder. Furthermore, a framegrabber card was added to a local computer system to allow RHEED images to be imported from either the S-VHS tape or from the CCD camera.

The second modification to the MBE system was necessary only for the second set of experiments. This modification was to retask the MBE system controllers to allow computer control of the Microwave power supply for the ECR source. Performing this task allowed for precise timing control of the Microwave power supply. Exact details of this modification are included for historical purposes in Appendix A.

The first group of experiments was a straightforward effort to understand the effect of the nitrogen plasma on the GaAs surface. In each of three growth runs, a GaAs surface was prepared by well-established methods. A 1 μm GaAs buffer layer was growth in each of the three runs. The buffer layers were deposited on semi-insulating Epi-Ready GaAs (100) substrates at temperatures of 590°C to 600°C. Growth rates were typically 1 ML/sec. After the buffer layers had been deposited, the MBE system was reconfigured to a state for the growth of GaN;

this merely requires the introduction of a stable nitrogen partial pressure at a level of 2.0×10^{-4} Torr. After the nitrogen partial pressure was established, a number of experiments were performed sequentially that involved the following steps: (1) The surface was given a timed exposure to the nitrogen plasma, at 100 W forward power; (2) An assessment was made of the condition and stability of the surface; (3) The surface was overgrown with GaAs. Note that in these experiments, there was no codeposition of Ga as the surface was nitrided. These experiments were repeated with incremental changes to a number of parameters including substrate temperature, exposure time, and As overpressure state. In each case, the RHEED images were recorded via the CCD camera to be studied in detail at a later time.

In the growth of the first set of samples, a mechanism of anion exchange was observed when the GaAs surface was exposed to the nitrogen plasma. Unfortunately, there was also a competing mechanism that appeared to be re-evaporation of the implanted nitrogen at the surface. In order to study this anion exchange in a quantitative way, it was conjectured that the nitrogen could be frozen in place if it were immediately buried by an overgrowth of GaAs. The amount of nitrogen implanted into the sample could then later be measured by means of High Resolution X-Ray Diffraction. In order to increase the signal level in the Rocking curves attained by this method of study, it was decided to grow GaN_yAs_{1-y}/GaAs periodic structures in which the GaN layer was presumed to be approximately 1 monolayer* and the GaAs spacer was consistently grown for 100 seconds at the Ga arrival rate which was effectively 0.75 ML/sec.

Originally, these structures were grown by a method which required manually engaging and disengaging the Microwave power supply for the nitrogen plasma. It was determined though, that manual control induced fluctuations beyond a tolerable level. The solution to this problem was to implement computer control over the microwave power supply. This led to the restructuring and retasking of the systems

---

*The origin of this assumption is based on the results from the Surface Nitridation experiments in the growth of the first set of samples.

control computers mentioned above. The exact details of this are included in Appendix A.

The substrates that were used for the growth of each superlattice sample were prepared in the growth chamber prior to deposition of the superlattices. The substrates for these samples were semi-insulating Epi-Ready GaAs (100) substrates. The oxides on these substrates were first thermally desorbed and then a buffer layer was deposited for each sample. The buffer layers were each approximately 1 μm of undoped GaAs and were grown under the same well-established conditions as were the buffer layers for each of the two previous sample sets. The parameters for the growth of these superlattices included the following. The microwave forward power driving the nitrogen plasma was in each case set to 100 W. Also, in each case it was observed that the reverse power was approximately 32 W. The nitrogen gas was in each case introduced into the system under identical conditions at a rate of 26 sccm.* Once this flow rate is established, the MBE system vacuum pumps were deliberately retarded so as to obtain a system pressure of 2.0×10^{-4} Torr. Furthermore, the Ga cell was set to a temperature of 1066°C. This temperature is known to produce an arrival rate equivalent to 1 ML/sec under GaAs growth conditions. However, under the high pressure of GaN growth conditions, there is an attenuation of approximately 25 to 28% due to scattering. In each sample growth, the Ga arrival rate was measured at the appropriate growth conditions.

The substrate temperatures were varied from 540°C to 580°C for this set of sample growths. The selection of the substrate temperature for each successive growth run was based on feedback from the previous growth experiments. In each experiment, the substrate temperature was chosen so as to maximize the incorporation of nitrogen into the samples. Extensive efforts were put forth to keep all other growth parameters the same. This required that each substrate be prepared and mounted by the same technique, and onto the same sample block for each growth experiment. Furthermore, efforts were made to always follow the same procedures

---

*As pointed out in Chapter 2, this flow rate suffers from an intrinsic error since the flowmeter used is calibrated for air rather than pure nitrogen. Despite the error this induces, the flow rate is highly reproducible.

in the *in situ* sample preparations and in the growth of the buffer layers. The chronological evolution of the substrate temperatures is shown in Table 3.1 on p. 52. For each sample in this set, a superlattice of 36 periods was grown. Each period of the superlattice consisted first of a nitrided monolayer. This monolayer was attained by means of a timed exposure of a GaAs surface to the nitrogen plasma. With the exception of the last sample grown in the series, the time of the exposures for each of the superlattice samples was 4 seconds; the time of the exposures for the last sample was 6 seconds. Immediately after the nitridation of the surface, the surface was overgrown with GaAs for 100 seconds at a typical growth rate of 0.75 ML/sec. After the growth of this GaAs spacer, the surface was allowed to "soak" under a flux of As_2 for 30 seconds before the growth of the next period of the superlattice. The purpose of this As "soak" was to allow the surface to relax and flatten before the next surface nitridation. Finally, upon completing the growth of the superlattice, a 500 Å GaAs cap layer was deposited on each sample. Furthermore, the evolution of RHEED images was recorded via the CCD camera for time periods representative of the growth. Upon removal of the samples from the MBE system, representative specimens were cleaved and shipped to have HRXRD studies performed. This experimental measurement provides a great deal of information about the actual structure that was grown.

3.3 RESULTS AND DISCUSSION

3.3.1 SURFACE NITRIDATION EXPERIMENTS

The RHEED images from the Surface Nitridation experiments yielded a great deal of both qualitative as well as quantitative information concerning the interaction of the nitrogen plasma with the GaAs (100) surface. From these findings, some direct inferences can be made concerning the stability of GaN under conditions similar to those employed in the previous chapter.

By exposing the GaAs surface to a brief exposure (5-10 seconds) of the nitrogen plasma, it was found that the transient (3 × 3) surface reconstruction pattern

Run Number	Sample Temperature (°C)	Time of Exposure (sec)
OS95.002	560	4
OS95.003	570	4
OS95.004	580	4
OS95.005	550	4
OS95.006	540	4
OS95.009	550	6

TABLE 3.1. Chronological evolution of superlattice growth parameters. All other growth parameters were nominally held constant.

was produced. Observing the RHEED patterns as the surface is nitrided is difficult because the nitrogen plasma displaces the RHEED beam. However, it is believed that the evolution from the (2×4) to the (3×3) surface reconstruction occurs in approximately 1 sec. The fact that the (3×3) RHEED images were attained simply by exposing the GaAs surface to the nitrogen plasma without the codeposition of Ga suggests that an anion exchange mechanism is occuring in which the As is replaced by nitrogen. Assuming that the (3×3) reconstruction pattern is the same as that which was observed in Chapter 2, this implies that the (3×3) RHEED pattern might represent some mixture of GaN and GaAs islands on the surface.

Perhaps as interesting as the (3×3) pattern itself is the stability of the (3×3) pattern. In the case of GaAs, a continuous overpressure of As is required when a sample is raised to high temperatures.[5] The exact overpressure of As that is necessary is a strong function of the substrate temperature. If this overpressure of As is interrupted, surface As is immediately evaporated leaving a Ga-terminated surface. This can be observed directly via RHEED; upon interruption of the As flux, the reconstruction immediately transforms from the As-stabilized (2×4) RHEED pattern to a Ga-stabilized (4×2) RHEED pattern. If the As flux is interrupted at elevated temperatures for as little as a few seconds, the sample will be irreparably damaged due to the loss of subsurface As.

In the case of the GaAs surface nitrided for a brief period of time the (3×3) surface reconstruction is observed to persistent, with or without the presence of an As flux, for at least 1 minute even at temperatures near 600°C. If the surface is allowed to decay in the presence of an As flux, it will decay into a rough, faceted GaAs surface with the As-stabilized (2×4) reconstruction over the course of one or two minutes. In the case of allowing the surface to decay without the As flux, a rough, faceted Ga-stabilized (4×2) reconstruction pattern is attained. Both of these results suggest that the implanted nitrogen is slowly evaporated, and in the presence of an As overpressure, the nitrogen is slowly replaced by As.

By using a frame grabber to acquire frames from the S-VHS recorded experiments, detailed quantitative information can be obtained from the RHEED images.

Shown in Fig. 3.1 on p. 55 is a plot of the intensity of the $\frac{1}{3}$ order diffraction line along the [110] direction as a function of time for a period before, during, and after a surface nitridation. To improve the signal to noise ratio, the intensity of the $\frac{1}{3}$ order line is integrated vertically. The time scale is chosen so that the nitridation of the surface begins at $t_0=0$ sec. In this particular example, the substrate temperature is 592 °C and the GaAs surface was nitrided for 3 seconds. As can be seen from the inset figure, the presence or absence of the As flux during the nitridation of the surface has little effect. However, the presence of the As flux after the surface is nitrided has a significant effect. Again, this is expected as from the discussion above, the presence of the As leads to a different final state of the surface after the re-evaporation or sublimation of the nitrogen. Note that the nitrided surface is manifestly more stable than a GaAs surface at these temperatures. This tends to imply that the top surface has little, if any, arsenic or GaAs islands as these would volatilize quickly, requiring a faster decay of the RHEED images.

It has been found that the decay in the presence of the As flux can be fit very well with the sum of two decaying exponentials of the form

$$I = A_s e^{-\frac{t}{\tau_s}} + A_l e^{-\frac{t}{\tau_l}} \quad . \tag{3.1}$$

In Eq. (3.1) τ_l and τ_s represent long and short decay times respectively. The rationale for the sum of the two decaying exponentials is that it is expected that surface and subsurface nitrogen will be evaporated at different rates as the nitrogen must diffuse through the lattice. The fit parameters have been found to be $\tau_s = 7.1$ seconds and $\tau_l = 48$ seconds. It would be interesting to plot the action of these fit parameters as a function of substrate temperature, in particular to see if the parameters would vary according to some Boltzmann factor with a constant activation energy. Unfortunately, at this time an insufficient volume of data has been accumulated to allow a plot with genuinely meaningful physical implications.

More interesting phenomena were observed for surfaces that were nitrided for short periods of time. In particular, it was found that commensurate, epitaxial GaAs could be deposited over the nitrided surface. High quality epitaxial GaAs could be obtained with as little as a few hundred angstroms of deposition. This
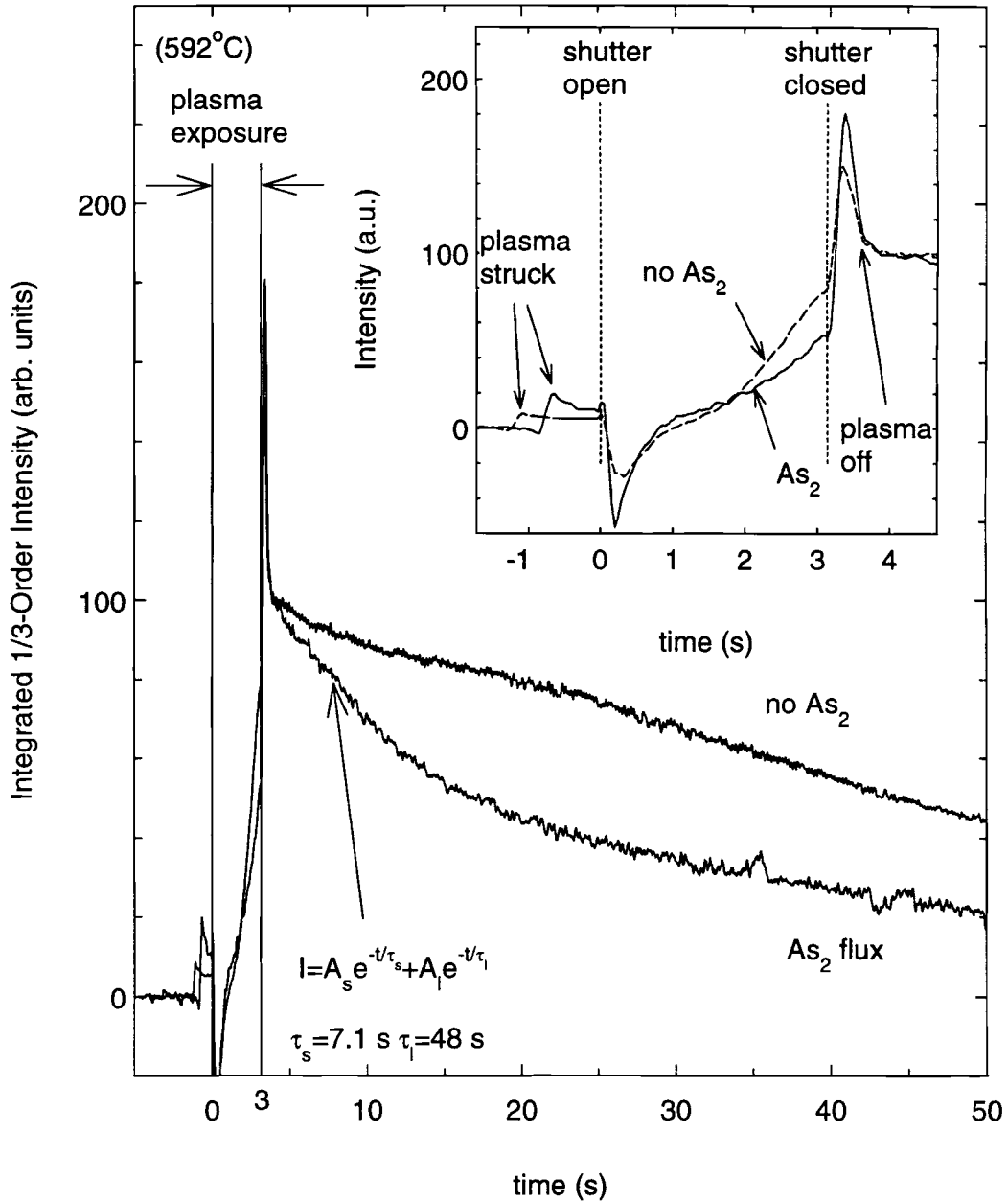
Figure 3.1. Shown is plot of the vertically integrated $\frac{1}{3}$ order RHEED streak intensity as a function of time for the period before, during, and after the nitridation of a GaAs (100) surface. The RHEED images were taken along the [110] direction. Shown in the inset is an enlargement of the plot for the time interval of the surface nitridation.

was observed experimentally using RHEED. This result actually verified that the superlattices that will be discussed in the next subsection could be grown. Furthermore, it was observed that the quality of the RHEED images improved more rapidly in the [110] direction than in the [1$\bar{1}$0] direction. This result suggests that preferential growth occurs along the [110] direction. Also, it was qualitatively observed that commensurate overgrowth of GaAs could only occur if the period of the surface nitridation was sufficiently short. While no quantitative study was made to determine a maximum allowable time of exposure, experimental work already suggests that exposures near 10 seconds are the greatest that can be endured and still allow overgrowth with high quality GaAs.

Again, by processing the RHEED images using a frame grabber and the recorded S-VHS tapes, information can be attained concerning surfaces that are exposed to the nitrogen plasma for too long. In this case of overexposure, a rough (1 × 1) surface reconstruction is obtained that is not commensurate with the underlying GaAs. In Fig. 3.2 on page 57, line scans perpendicular to the RHEED streaks are presented for three distinct RHEED patterns each under the same RHEED imaging conditions. Curve (a) corresponds to the GaAs 2× pattern observed along the [110] direction. Curve (b) corresponds to the transient 3× pattern and (c) is taken from the spotty 1× pattern obtained by overexposing the sample surface to the nitrogen plasma. By considering the position of the ±1 order streaks, it can be seen that the surface yielding the (3 × 3) RHEED pattern is commensurate with the underlying GaAs while the surface exhibiting the (1 × 1) pattern clearly is not. By plotting in units of the surface wave vector, it is possible to discern the in-plane lattice parameters of the nitrided surface. By letting the space between the ±1 order streaks of the GaAs 2× pattern be b, it is found from the plot in Fig. 3.2 that the separation of the ±1 order streaks of the spotty (1 × 1) pattern is 1.3b. This implies that

$$1.3 \times \frac{2\sqrt{2}\pi}{a_{\parallel}^{\text{GaAs}}} = \frac{2\sqrt{2}\pi}{a_{\parallel}^{(1\times1)}} \tag{3.2}$$

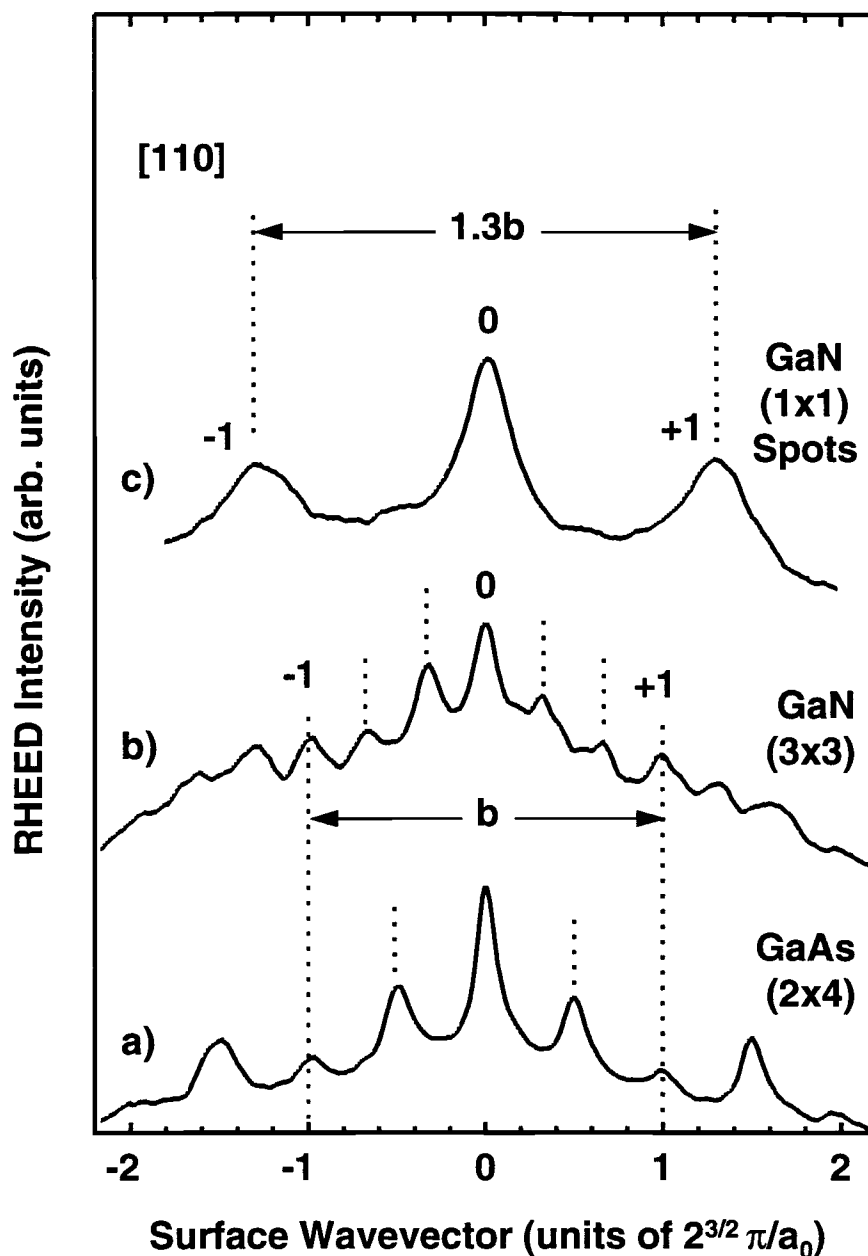Figure 3.2. Shown are plots of horizontal lines scans of (a) the GaAs $2\times$ image before surface nitridation, (b) the $3\times$ image attained by nitriding for 5 sec, and (c) the spotty $1\times$ pattern produced through exposure to the nitrogen plasma for 1 minute. All scans are along the [110] direction under identical imaging conditions. Scans are plotted in units of the GaAs Surface Wave Vector.

where in Eq. (3.2) $a_{\parallel}^{GaAs}$ is the in-plane GaAs lattice parameter, and $a_{\parallel}^{(1\times1)}$ is the in-plane lattice parameter for the spotty (1×1) structure. This implies that $a_{\parallel}^{(1\times1)} = a_{\parallel}^{GaAs}/1.3$. Calculation of this yields $a_{\parallel}^{(1\times1)} = 4.3$ Å. This result, within experimental error, is in agreement with the lattice parameter for GaN which is known to be 4.52 Å.

3.3.2 GaN_yAs_{1-y}/GaAs SUPERLATTICE EXPERIMENTS

3.3.2.1 <u>RHEED</u>. The RHEED images that were observed in the growth of the superlattices exhibited a similar sequence of patterns as were observed in the Surface Nitridation studies in the previous section. Interestingly enough though, the evolution of the RHEED images exhibited a strong temperature dependence in the rate of this evolution. The evolution of images is as follows. Prior to the surface nitridation, the GaAs surfaces exhibited the characteristic $2\times$ diffraction pattern of an As-terminated GaAs surface. Upon initiation of the surface nitridation, the effect of the nitrogen plasma upon the RHEED beam distorted the RHEED images to such a degree that it was impossible to make valid observations. At the initiation of the GaAs overgrowth, the $3\times$ diffraction pattern is observed. With the successive deposition of the GaAs, the $\pm\frac{1}{3}$ and $\pm\frac{2}{3}$ order lines decreased in intensity while the intensity of the $\pm\frac{1}{2}$ order lines increased from the background level forming the characteristic $2\times$ pattern. Note that in this evolution, the ±1 order lines are believed to remain in a constant position indicating that the nitridated layer is commensurate with the GaAs spacer layers. The time scale of the evolution of the $3\times$ pattern into the $2\times$ pattern is strongly dependent on temperature. At higher temperatures, it is observed that the $\pm\frac{1}{3}$ and $\pm\frac{2}{3}$ order lines are more persistent. Alternatively, at lower temperature, the $3\times$ pattern gives way almost immediately to the characteristic $2\times$ pattern for GaAs.

Presuming that the (3×3) pattern is indicative of a highly-strained GaN surface with little surface As, then the temperature dependence of the evolution of RHEED images implies that upward segregation of implanted nitrogen is occuring. Recall that because of the high strain in the lattice due to the nitrogen, it is likely

energetically favorable for the nitrogen atoms to move or segregate upward rather than being overgrown by GaAs. At higher temperatures, it is expected that segregating elements would be more mobile and would therefore be present in the moving growth surface for a greater period of time. This is exactly the observed phenomenon; the $3\times$ pattern is more persistent at higher temperatures. The opposite holds true for lower temperatures also.

3.3.2.2 X-RAY DIFFRACTION.

The data attained from the $\Omega/2\theta$ Rocking curve scans were first modeled using software provided by Philips Analytical Instruments. The software generates the expected Rocking curve by means of a dynamic simulation based on the Tagaki-Taupin equations. An example of the simulated Rocking Curves generated by this software is shown is Fig. 1.8 on p. 22. In each case, the simulation closely matched the observed Rocking curves. The peak positions and the diffraction orders from the data were processed again using the simple procedure described in Chapter 1 to determine the equivalent monolayer composition of nitrogen. It was found that the $\Omega/2\theta$ Rocking curves obtained from the superlattice samples also exhibit a strong temperature dependence as did the RHEED patterns. Examples of the Rocking Curves are shown in Fig. 3.3 on p. 60. The data shown in the figure exhibits a clear temperature dependence. The nitrogen incorporation into the sample is indicated by the separation of the sample peak from the GaAs (400) substrate peak and by the persistence of satellite peaks. The superlattices grown at lower temperatures exhibit a greater monolayer equivalent incorporation of nitrogen than those grown at higher temperatures. Table 3.2 on p. 61 presents the same information as Table 3.1 as well as the monolayer equivalent incorporation of nitrogen for each sample in the set. This table shows the effect of parameter variations on the nitrogen composition of the superlattice samples. Also, rather than appearing chronologically, this table is ordered according to the nitrogen composition of the samples.

An Arrhenius plot of the monolayer equivalent composition of nitrogen, y, versus 1000/T and temperature is given in Fig. 3.4 on p. 62. In this figure, two
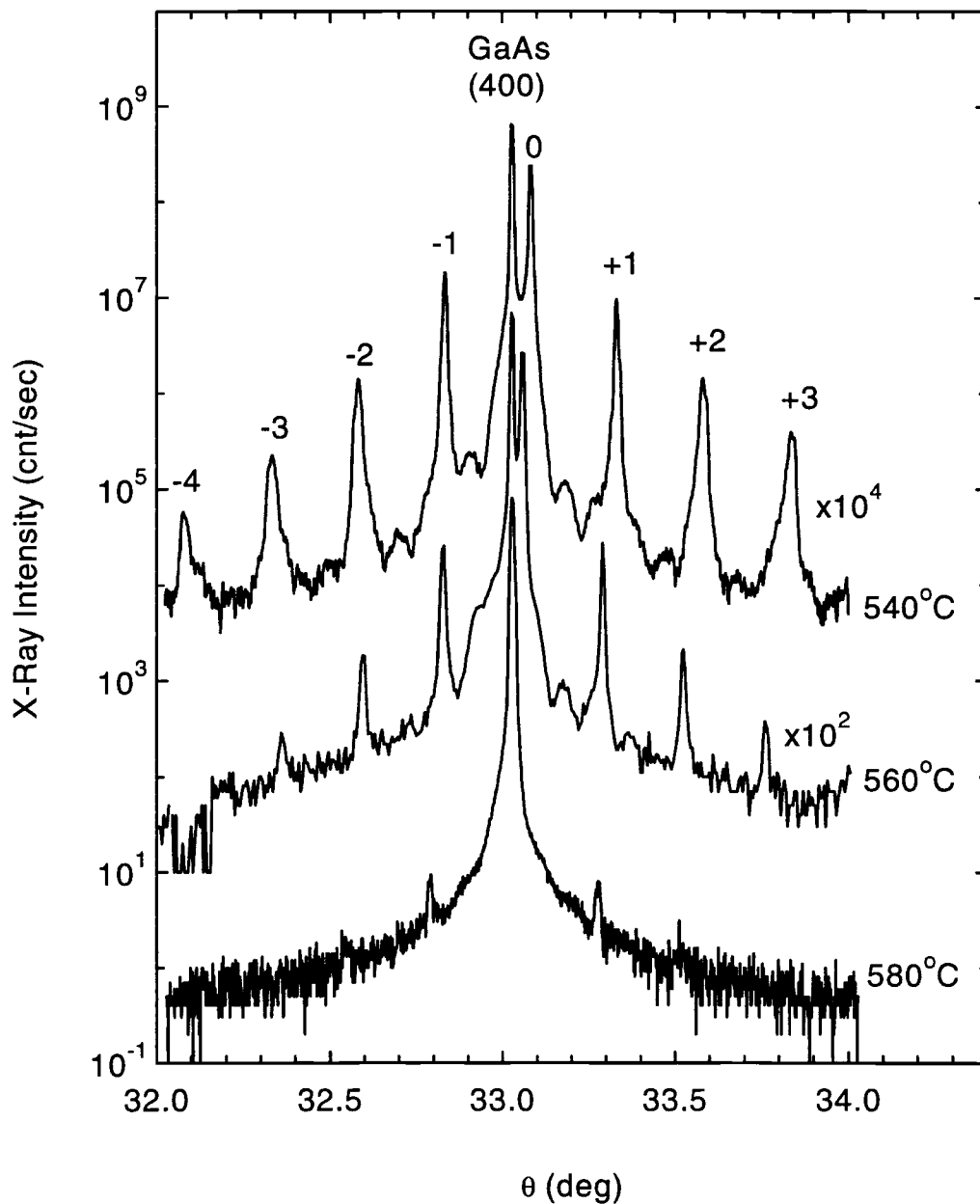
Figure 3.3. Presented are representative Rocking Curves or $\Omega/2\theta$ style X-Ray Diffraction scans for several of the superlattice samples. Clearly the nitrogen incorporation is strongly dependent on the growth temperature. Successive scans are veritcally offset by a factor of 100 for clarity.

Run Number	Sample Temperature (°C)	Time of Exposure (sec)	Nitrogen Composition (%)
OS95.004	580	4	4
OS95.003	570	4	7
OS95.002	560	4	16.5
OS95.005	550	4	26
OS95.006	540	4	26.5
OS95.009	550	6	33

TABLE 3.2. Presented in the table above are the parameters that were varied in the growth of the superlattice samples. The table clearly shows the strong temperature dependence of the monolayer equivalent nitrogen composition on the sample growth temperature as well as the time of exposure.
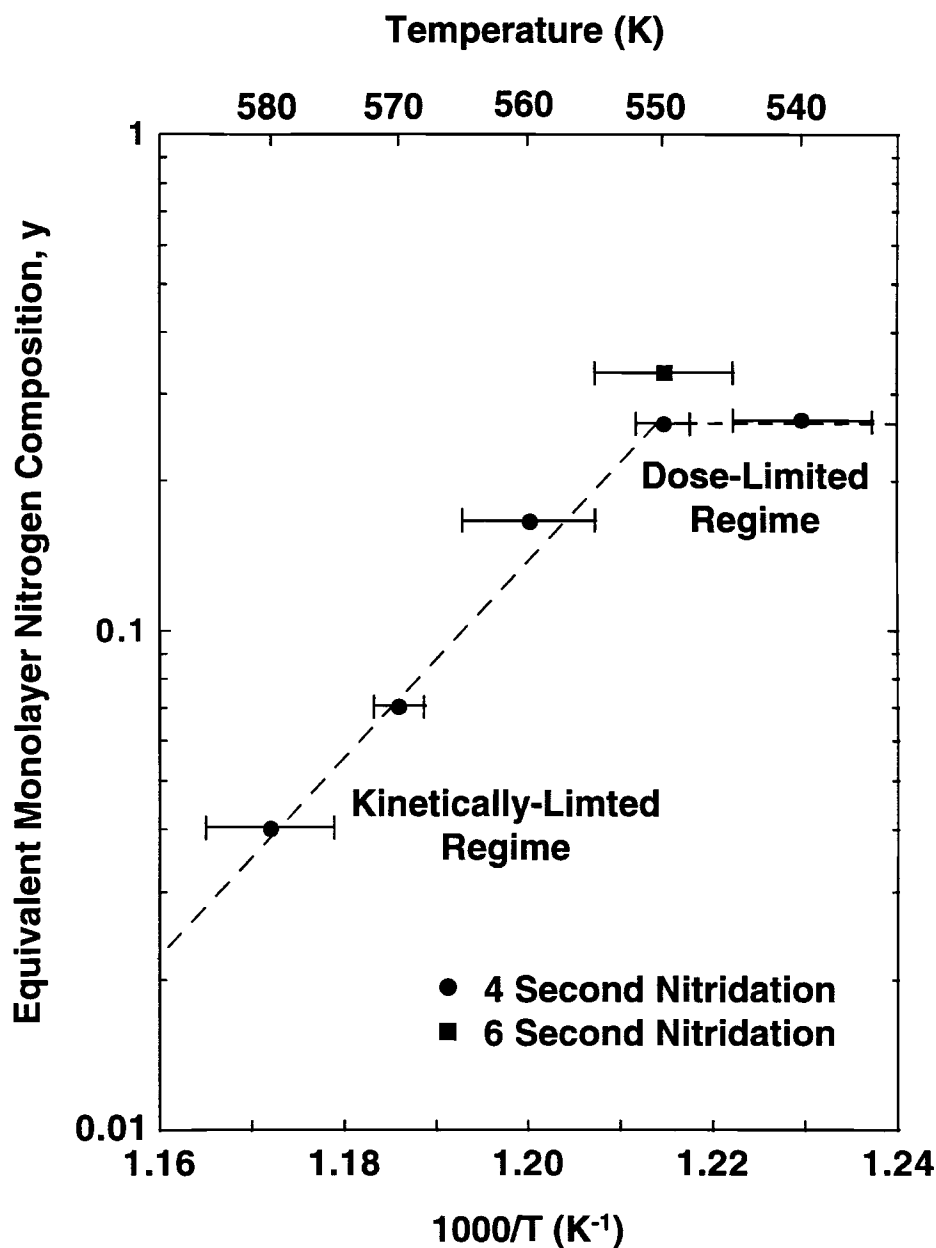
Figure 3.4. Presented is an Arrhenius plot of the equivalent monolayer nitrogen
composition of the superlattice samples versus T along the top axis
and 1000/T along the bottom axis. Both a kinetically-limited linear
regime and a flat dose-limited regime can be observed.

distinct regimes can be observed. First, there is a linear regime or a regime in which the nitrogen incorporation into the sample is decreasing with increasing temperature. This is labeled as the kinetically-limited regime in the figure. As the nitrogen incorporation of the sample is nearly linear on the Arrhenius plot, this suggests that the nitrogen incorporation is limited in this temperature region by the kinetic processes observed in the sample growths, that is by the segregation of implanted nitrogen to the surface and re-evaporation of this nitrogen.

Also in Fig. 3.4 there is a flat or nearly constant composition regime. Since the nitrogen incorporation is nearly constant in this temperature regime, this suggests that at lower temperatures, the incorporation of nitrogen into the superlattice samples is not limited by the observed thermally activated processes of nitrogen segregation and surface re-evaporation. The one sample, OS95.009, which was grown using a longer plasma exposure time resulted in a sample with approximately 27% more nitrogen incorporated into each monolayer. This suggests that in the low temperature regime, the amount of nitrogen in each nitrided monolayer of the superlattice is limited by the time of exposure to the nitrogen plasma or the dose that was provided. For this reason, the lower temperature regime is labeled as a dose-limited regime in Fig. 3.4.

3.4 CONCLUSIONS

In this chapter, several notable discoveries have been presented. In the Surface Nitridation studies conducted on the first group of samples, a number of important properties were observed of both the interaction of a GaAs surface with a nitrogen plasma and the stability of GaN surfaces formed by nitridation of a GaAs surface.

Upon a brief exposure to a nitrogen plasma, the GaAs (2×4) surface reconstruction is replaced by a (3×3) surface reconstruction. Based on the stability of this surface reconstruction, which persists an order of magnitude longer in time than that of GaAs under similar conditions, it was determined that the (3×3) reconstruction must be composed almost exclusively of GaN. Since it was also shown

that this GaN monolayer is commensurate with the GaAs subsurface layers, it is reasonable to believe that the (3×3) surface reconstruction is caused by high levels of strain in the nitrided monolayer. To be certain of this, it would be necessary to perform detailed theoretical calculations to determine if this is reasonable.

It was noted that the effect of an As partial pressure during the nitridation of a GaAs surface had little effect on the surface that was formed. However, the As partial pressure had a dramatic effect on the post-nitridation evolution of the GaN monolayer. It was found that the decay of the GaN surface under an As partial pressure can be explained reasonably well as the replacement of surface and subsurface nitrogen with arsenic. A study of the temperature dependence of this mechanism could be quite interesting, but the data for such a study is not available at this time.

Furthermore, it was shown in the Surface Nitridation experiments that these nitrided monolayers of GaN could be commensurately overgrown with GaAs, and that high quality GaAs could be attained with as little a few hundred angstroms of deposited GaAs. Still another phenomenon observed is that there exists preferential ordering along the [110] direction during the GaAs overgrowth. This is consistent with the long established theory that GaAs grows preferentially along the [110] direction. This is the most commonly offered explanation for observing RHEED oscillations most easily in the [110] direction.

When the GaAs surfaces were nitrided for more than approximately 10 seconds, it was found that a spotty (1×1) surface reconstruction was attained. The (1×1) spots in this reconstruction were shown to not be commensurate with the underlying GaAs. Furthermore, digital analysis of the spacings of these spots in the RHEED images indicated that within experimental error, the surface exhibited the same in-plane lattice parameter as that of zincblende GaN. Another interesting observation was that this surface could not be overgrown with high quality GaAs.

The observation that the nitrided GaN monolayers could be commensurately overgrown with GaAs suggested that the surface kinetics could be studied more extensively by growing GaN_yAs_{1-y}/GaAs superlattice structures and employing High-Resolution X-Ray Diffraction. In the growth of the GaN_yAs_{1-y}/GaAs structures, it was observed that there was a temperature dependence both on the monolayer equivalent composition of nitrogen, y, and the persistence of the $3\times$ RHEED diffraction lines during the overgrowth of nitrided surfaces with GaAs. This temperature dependent persistence of the $3\times$ pattern strongly suggests that there are thermally activated processes such as segregation of the nitrogen and re-evaporation (sublimation) of nitrogen during the overgrowth. Again, agreement between a physically reasonable theoretical model and experimental results would strongly reinforce the proposed kinetic mechanisms.

Furthermore, it was observed that two distinct regimes existed in the plot of the monolayer equivalent nitrogen composition versus the substrate temperature. For the higher temperature regime, it was found that the nitrogen incorporation was limited by the thermally activated kinetic processes occuring at the surface. Furthermore, it was found that the percent nitrogen incorporation could be nicely fit to an Arrhenius style plot over the appropriate temperature range. For the lower temperature regime, it was found that the incorporation of nitrogen was limited by the time of exposure to the plasma or the dose. This explanation for the behavior in this regime is further supported by the single growth experiment conducted using a longer exposure time.

CHAPTER 4

SUMMARY AND CONCLUSIONS

In Chapter 1, a number of introductory items were presented. First, the technological importance of GaN was discussed. Briefly, GaN is currently being pursued for application in opto-electronic devices. The wide, direct bandgap of GaN makes it potentially useful in devices such as LED's and laser diodes operating from the ultraviolet to the blue-green portion of the electromagnetic spectrum. Also, the mechanical rigidity and thermal stability of GaN make it a desirable semiconductor for use in other opto-electronic devices.

Also, in Chapter 1, Molecular Beam Epitaxy and Electron Cyclotron Resonance Plasma-Assisted Molecular Beam Epitaxy were introduced. A brief description was given of the principal components that comprise MBE and ECR-MBE systems and of the physics behind some of these components. Furthermore, a discussion was given of the physics of epitaxial growth by MBE. In particular, a discussion was given showing why simple thermodynamic principles force epitaxial growth to occur.

The most important *in situ* and *ex situ* characterization techniques were introduced in Chapter 1. In particular, Reflection High Energy Electron Diffraction (RHEED) was presented. A brief discussion was offered showing how the Ewald construction may be applied to this *in situ* characterization. Also, High Resolution X-Ray Diffraction was introduced in Chapter 1. A discussion was given showing how this *ex situ* characterization technique is used to determine the structure and composition of simple superlattice samples.

Presented in Chapter 2 were the results of a set of experiments aimed at growing epitaxial GaN films on GaAs (100) substrates. One objective of this set

of experiments was to determine the optimal conditions for the growth of epitaxial zincblende films of GaN. Two important growth parameters, the Ga arrival rate and the forward nitrogen plasma power were varied in successive steps to optimize the growth conditions. In each successive growth experiment, one of the two parameters was "tweaked" in an effort to improve the growth of GaN epitaxial films. One other important growth parameter, the substrate temperature, was not varied throughout the growth of this sample set in order to simplify the optimization procedure and reduce the number of growth experiments.

In performing this set of experiments, a number of interesting observations were made. First, it was observed that at the initiation of GaN growth, the RHEED images evolved through a specific sequence of surface reconstruction patterns. Observed first in this sequence, prior to the initiation of growth, was the (2×4) surface reconstruction associated with an As-terminated GaAs surface. Immediately upon initiation of GaN growth, the RHEED patterns shifted to a (3×3) surface reconstruction. With the continued deposition of GaN, the RHEED patterns evolved to a very spotty (2×2) pattern. The spottiness of this pattern indicates that the surface is microscopically rough and faceted. With continued deposition, the RHEED images evolved to a smooth, streaked (2×2) pattern. In the experiments that were successful in growing GaN epitaxial films of relatively high quality, the RHEED patterns were eventually observed to indicate (2×4) surface reconstruction patterns. Furthermore, the diffraction lines of this (2×4) and the (2×2) RHEED patterns were further separated than the diffraction lines of the GaAs (2×4) and the transient (3×3) RHEED images. These more widely spaced diffraction lines are consistent with imaging a material that has a smaller lattice parameter. It is interesting to note that one of these RHEED patterns, the (3×3), had not previously been reported in any professional publication.

In the growth experiments discussed in Chapter 2, a mode by which the growth of GaN is self-limited was observed. This mode appears to be caused by a Ga arrival rate that is excessive when compared to the arrival rate of the species

of nitrogen that is responsible for growth. The result of this mode of self-limited growth is that the growth surface becomes coated with Ga.

Finally, in Chapter 2, growth experiments suggested that a functional set of growth parameters for the growth of zincblende GaN on GaAs (100) substrates included (1) a substrate temperature of 620°C, (2) a Ga arrival rate of 0.05 ML/sec under GaAs growth conditions, and (3) a Microwave forward power of 100 W. While these growth parameters were proven to be functional, it was clear that they were not optimal. Two of the particular problems with this set of growth conditions include: (1) the extremely low growth rate, and (2) the deposited GaN films never becomes smooth on a microscopic scale, when compared to GaAs samples.

The observed RHEED images of the previous set of growth experiments as well as the modes of self-limited GaN growth suggested that more needed to be understood about the interaction of the nitrogen plasma with the GaAs surfaces as well as the characteristics of the nitrided surfaces under growth conditions. These characteristics were investigated by two sets of growth experiments in Chapter 3.

In the first set of these sample growths, it was determined that the GaN surface attained by nitriding a GaAs surface for a short period of time was extremely stable even at high temperatures. Furthermore, observations of the decay of such nitrided surfaces indicated that a temperature dependent nitrogen re-evaporation phenomenon was taking place. A study of the kinetics of this re-evaporation phenomena was conducted. This kinetics study suggested that both surface and sub-surface evaporation of nitrogen was taking place. Further, the stability of the nitrided surface indicated that it was composed of a very small percentage of As. From this, it was inferred that a short nitrogen plasma exposure of the surface resulted in a nitrogen-for-arsenic anion exchange in which the top surface As was completely replaced with nitrogen. Also, it was inferred from this study that the observed (3 × 3) surface reconstruction could have in fact been attributable to a highly strained GaN monolayer at the top surface of the sample. To confirm this, it will be necessary to perform detailed theoretical calculations.

Furthermore, it was observed in these sample growths that GaN surfaces formed by short nitrogen plasma exposures could be commensurately overgrown with GaAs. This was to be expected as RHEED studies of the (3 × 3) surface reconstruction indicated that it was commensurate with the GaAs surface. Longer exposures of the GaAs surface to the nitrogen plasma resulted in a rough, faceted surface with a lattice parameter which was, within experimental error, that of bulk zincblende GaN.

The fact that GaAs surfaces that were briefly exposed to the nitrogen plasma could be commensurately overgrown with GaAs led to a second set of growth experiments. In this set of sample growths, the temperature dependence of the re-evaporation of nitrogen was studied. The RHEED images observed during the growth of these superlattice samples suggested that a segregation phenomenon was occuring during the overgrowth of GaAs as well as the re-evaporation. Detailed X-Ray Diffraction $\Omega/2\theta$ style Rocking curves were attained for each sample. Analysis of this data yielded the monolayer equivalent composition of nitrogen. This showed that the re-evaporation of nitrogen from the surface exhibited a strong temperature dependence. It was learned that for short plasma exposures the monolayer equivalent composition of nitrogen was limited in one of two ways depending on the temperature of the sample growth. First, it was found that for higher temperatures, there was a lesser amount of nitrogen in the superlattices and the nitrogen incorporation into the samples could be fit nicely to an Arrhenius plot in this temperature regime. This implied that the nitrogen incorporation into the sample was being limited by the thermally activated processes of segregation and surface re-evaporation of nitrogen that were observed. Second, it was found that at lower temperatures, the incorporation of nitrogen into the samples was higher and largely independent of temperature. This implied that the thermally activated processes of segregation and re-evaporation were much less active at these lower temperatures. Furthermore, one sample was grown with a longer exposure time than the others in this sample set. The higher nitrogen incorporation of this sample suggested that in this lower temperature regime, the incorporation on nitrogen into the sample was

limited by the exposure of the sample to the nitrogen plasma or the dose that the sample was given.

Finally, the various results that have been obtained through the study of the three sets of growth experiments can be used to predict the necessary corrections to make to the growth conditions for the growth of high quality epitaxial zincblende GaN on GaAs (100) substrates. As pointed out earlier in this chapter, the two most severe difficulties with the set of growth parameters that were established through the work in Chapter 2 are (1) the growth rate is too slow, and (2) the surface is too rough. In order to correct for surface roughness, it is necessary raise the substrate temperature to allow for a higher degree of mobility for atoms at the surface. However, from the results attained in Chapter 3, it is known that this will cause a faster rate of re-evaporation of nitrogen from the surface. To compensate for this faster rate of nitrogen loss from the sample, it will be necessary to increase the flux of the species of nitrogen that is responsible for growth. Also, to increase the growth rate, the arrival rate of Ga must be increased. It was learned through the work presented in Chapter 2 that an increased Ga arrival rate results in a surface that is coated with Ga unless a sufficient flux of the nitrogen species responsible for growth is available. While it will still be necessary in the future to optimize the nitrogen source gas flowrate and the pressure in the growth chamber in order to optimize the ECR source for the production of the species of nitrogen that is responsible for growth, it is expected that an increase in the power of microwaves that are provided to the ECR source will be necessary to attain a greater flux of the nitrogen species that is responsible for growth. Based on the work presented in this thesis, it can be concluded that in order to grow high quality films of epitaxial zincblende GaN, higher growth temperatures and higher arrival rates of suitably activated nitrogen species will be essential.

BIBLIOGRAPHY

1. Bhargava, R. N.; Journal of Crystal Growth 117 (1992) 894-901.

2. Shuji Nakamura, Takashi Mukai, and Masayuki Senoh, Appl. Phys. Lett. 64(13) 1687 (1994).

3. Compound Semiconductor 1(1) 34 (1995).

4. S. Strite and H. Morkoç, J. Vac. Sci. Technol. B. 10(4) 1237 1992.

5. Parker, E. H. C., "The Technology and Physics of Molecular Beam Epitaxy", Plenum Press, London (1985).

6. Cho, A. Y., "Key Papers in Applied Physics: Molecular Beam Epitaxy", AIP Press, Murray Hill, NJ. (1994).

7. Callen, H. B., "Thermodynamics and An Introduction to Thermostatistics", John Willey & Sons, New York (1960).

8. J. H. Neave, and B. A. Joyce., Journal of Crystal Growth 45, 302 (1978).

9. J. H. Neave, and B. A. Joyce., Journal of Crystal Growth 44, 387 (1978).

10. Asmussen, J.; "Instruction Manual: Wavemat Microwave Plasma Disk Reactor", Wavemat, inc., Plymouth, MI 1993.

11. "Model MPDR 610iA Microwave ECR Plasma Ion Source", Wavemat, inc., Plymouth, MI 1993.

12. A. Y. Cho, J. Appl. Phys. 42(5) 2074 (1971).

13. A. Y. Cho, J. Appl. Phys. 41(7) 2780 (1969).

14. Kittel, C; "Introduction to Solid State Physics", John Wiley & Sons, Inc., New York, sixth edition (1986).

15. Ashcroft, N. W., Mermin, N. D.; "Solid State Physics", Holt, Rinehart, and Winston, New York (1976).

16. Sandin, T. R., "Essentials of Modern Physics", Addison-Wesley, Reading, Mass. (1989).

17. Serway, R. A., Moses, C. J., Moyer, C. A.,"Modern Physics", Harcourt Brace Jovanovich College Publishers, Orlando, Fl. (1989).

18. "Quadrex 200 Residual Gas Analyzer Technical Manual", Leybold-Inficon, 1989.

19. Cullity, B. D.; "Elements of X-Ray Diffraction", Addison-Wesley, Reading, Mass. (1956).

20. C. R. Wie, J. Appl. Phys. 66(2) 985 1989.

21. V. S. Speriosu and T. Vreeland, Jr. J. Appl. Phys 55(6) 1591 (1984).

APPENDICES

APPENDIX A

MBE SYSTEM MODIFICATIONS

A.1 ECR PLASMA SOURCE GROWTH AND BAKEOUT INTERLOCKS

The Electron Cyclotron Resonance Plasma Reactor that is used in the growth of GaN requires an external source of clean, pressurized air for cooling. The pressurized air must be supplied at a rate of at least 3 cubic feet per minute to the ECR source during operation and for 30 minutes after use. The cooling gas maintains the ECR source at a relatively low and stable temperature during operation. This is necessary for the following three reasons. First, a relatively constant temperature for the ECR source during operation is necessary to stabilize the resonance cavity that is essential to the operation of the ECR source. Second, a low temperature is necessary to protect the magnets in the ECR source. As these are ferromagnets, heating will lead to a loss of the magnetic field strength of the various magnets in the assembly. According to the ECR Operation Manual, these magnets should *never* be heated above 150°C. Lastly, a relatively low temperature is necessary to protect the metallic seal that joins the alumina plasma cup to the surrounding stainless steel parts. Excessive heating of this seal could result in a cataclysmic loss of vacuum.

Given the importance of the cooling gas to the ECR source and to the MBE system, it was deemed necessary to modify all of the MBE system interlocks that would be active at a time in which the ECR is in use or may be heated. This required that a modification be made to the bakeout interlock and that a new interlock be built to protect the ECR plasma source during growth.

For either interlock, the desired protection is that the source of heat for the ECR plasma reactor be interrupted in the event of an insufficient supply of cooling gas. To maintain the necessary 3 cfm cooling gas flowrate, it is necessary to have a net positive pressure of 15 psi relative to the air pressure in the lab. A standard pressure switch was attained featuring a variable pressure crossover. The pressure crossover was set to approximately 10 to 12 psi. Though a DPST switch, the pressure switch is used in a "normally-open" configuration for both interlocks. This pressure switch was installed on the cooling gas supply side of the ECR as close to the ECR source as was practical. The diffuse nature of the cooling gas outlet holes made it impossible to install the pressure switch on the return side of the ECR source. The cooling gas is attained by using a high density filter and a single-stage pressure regulator to condition the house-supplied compressed air.

The MBE system has a series of pressure and temperature interrupts associated with the bakeout interlock. Each interrupt consists of an SPST switch that is actuated by either a pressure or temperature reading; each SPST switch is connected in series. A small AC current is driven through the series of switches by the first power distribution on the MBE system (located between the pneumatic shutter interface and the sorbtion pumps). If there is an interruption of the current flow through the switches, then the power distribution will fail to drive the MBE system bakeout heaters.

The modification to the bakeout interlock was the inclusion of the pressure switch mentioned above in series with the other interrupt switches. Physically, there is a standard automotive 4-wire connector located in the lowest cable tray on the right-hand side of the console as viewed from the rear. In order for the bakeout interlock condition to be satisfied, the cable connected to the pressure switch must be plugged into the connector which is located in the cable tray and a 15 psi pressure must be supplied to the ECR source.

The growth interlock that was constructed to protect the ECR is much simpler than the bakeout interlock. The ECR microwave power supply has a built-in interlock. It is necessary that two pins, I1 and I3 on the terminal block, be shorted

together in order for the ECR microwave power supply to be engaged. A 4-wire connector compatible with the cable on the pressure sensing switch was attached to the terminal block on the ECR microwave power supply so that the pins were shorted only when there is sufficient pressure to actuate the pressure switch.

A.2 MICRISTAR/DIMENSION CONTROL OF EFFUSION CELLS AND THE ECR POWER SUPPLY

As mentioned in the text of the thesis, it was necessary to modify the process control computers that are used to control the MBE system to allow for precise timing control of the ECR microwave power supply. Essentially, the MBE system uses four separate process control computers; these are the three Micristar controllers and the Dimension controller. These process control computers are highly specialized controllers designed for applications such as MBE. Each of the Micristars is capable of controlling two regulated devices, usually effusion cells; one of the Micristars, Micristar #3, controls the eight source flange shutters. The Dimension is essentially a more modern, more flexible, and more powerful version of the Micristars. It is capable of controlling four devices and twelve shutters, simultaneous to monitoring twelve user defined alarms.

The Dimension controller was added to the MBE system when the MBE system was upgraded for performing Electron Cyclotron Resonance Plasma-Assisted Molecular Beam Epitaxy. After completion of that upgrade, the three Micristar controllers were used to regulate the cell temperatures of the As bulk evaporator, the As cracker, the Al effusion cell, the Ga effusion cell, the In effusion cell, and the sample heater. Furthermore, the Dimension controller was used to control the Si effusion cell and the Mg cell.

Each of these process controllers allows the execution of user entered programs so that cells may be ramped to specific temperatures in a consistent and uniform manner. Also, by programming Micristar #3, it is possible to control the growth of many structures since this controller also controls the source flange shutters. In particular, programs for the growth of the superlattice samples grown for

the work in Chapter 3 were written and executed on this controller. As Micristar #3 controlled the growth of the superlattice samples, it was clear that this controller should be used to control the ECR microwave power supply. It was necessary that this Micristar have control of the ECR as this would allow the superlattices to be grown by executing a single program on a single Micristar. By using a single program, difficulties associated with synchronizing the execution of multiple programs are avoided.

Prior to the modifications described here, Micristar #3 controlled the As bulk evaporator and the As cracker. Since the Micristars could only regulate two devices, the control of the As cracker was transfered to the third channel of the Dimension. The Dimension was configured to accept an analog input from the thermocouple of the As cracker; this was done by changing jumper settings on the device card as instructed by the Dimension User's Manual in Chapter 2, pages 2-4 and 2-5. Furthermore, the analog input was configured in software to be interpreted as a thermocouple. The terminals of the analog input defined as the thermocouple were shorted together, and an offset was added to the thermocouple reading, so that the temperature of the As cracker always read as 0°C on the Dimension. The additive offset was necessary to defeat the Dimension's scheme of cold junction compensation for thermocouples. The analog output signal from the Dimension was connected to the Sorensen power supply that powers the As cracker. The rate and reset parameters for the third output channel of the Dimension were set to zero. Finally, the gain parameter for channel #3 of the Dimension was set so that a temperature setpoint of X for the As cracker, resulted in an X percent output from the Sorensen power supply. Historically, the As cracker has always been controlled using a similar scheme.

Micristar #3 needed to be configured to control the ECR microwave power supply. The thermocouple terminals of the open Micristar channel were shorted together. This caused the thermocouple reading for that channel to read 0°C. The ECR microwave power supply accepts at the front panel a remote signal to control the forward microwave power to the ECR source. The output signal from channel 2

of Micristar #3 was connected to remote signal input by means of a BNC cable. A BNC bulkhead was installed in the rear of the MBE system console in the locality of Micristar #3. Furthermore, the rate and reset parameters for this channel of the Micristar controller were set to zero. The gain parameter was adjusted so that a temperature setting of X degrees on the Micristar resulted in a forward power level of X watts. This scheme worked efficiently to control the ECR microwave power supply in a manner that was simple for the user.

It is important to note that there is a performance limitation of this scheme for controlling the ECR microwave power supply. The forward power output of microwaves from the ECR power supply will vary proportionally from 0 to 300 watts as the input signal varies from 0 to 10 volts. The analog output of the Micristar varies from 0 to 5 volts depending on the output level determined by the Micristar. As a consequence of this, the Micristar can be programmed to deliver at most 150 watts of microwaves to the ECR plasma source. For this to be corrected, the Micristar will need to be reconfigured.

A.3 SAMPLE TRANSFER SYSTEM

The OSU MBE system utilizes a sample transfer rod assembly to move samples into the growth chamber. Two sample blocks may be loaded into an elevator in the introductory chamber which may be vented independently of the other chambers. Once the introductory chamber is pumped down to a suitable vacuum level, these sample blocks may be loaded onto the sample transfer rod, and may then be transfered into the growth chamber. The transfer rod used in this process is comprised of a long cylindrical stainless steel sheath which encases a long metal rod. The long metal rod within the sheath is magnetically coupled to a magnet external to the vacuum environment which slides on the stainless steel sheath. This magnetic transfer rod provided a means of locomotion for samples in the vacuum system. This transfer rod is supported by a small set of rollers or bearings that act as a pivot point while the transfer rod is extended into the growth chamber.

The long length of travel of the transfer rod (approximately 3.5 feet) causes large forces to be applied to the pivot point when the transfer rod is fully extended.

The growth stage that holds the sample blocks requires that the sample blocks be positioned very precisely while being loaded; tolerances for this positioning are only a few millimeters. The need for precise positioning and the long extension of the transfer rod while samples are loaded causes the sample transfer mechanisms, and the sample transfer rod in particular, to be extremely sensitive. As a result of this sensitivity, even the most minor accidents typically result in a transfer rod that is too poorly aligned to load samples. In several instances, misalignment of the transfer rod has caused damage to the delicate mechanical parts of the growth stage.

To provide additional support, a block with three bearings or rollers was installed in the growth chamber so that the end of the fully extended sample transfer rod would roll onto the support block as it was inserted into the growth chamber. This support block was installed in the growth chamber prior to the delivery of the MBE system to OSU. By virtue of its position, the support block applied pressure from below to the lowest points on the transfer rod. Unfortunately, the lowest points were two large mounting screws with rounded heads. The rounded heads caused the rolling of the transfer rod over the bearings of the support block to be quite bumpy. This bumpiness in the transfer of samples contributed to misalignment of the transfer rod as well as significantly complicating the realignment procedure.

It was determined that to prevent frequent and repetitive ventings of the growth chamber to repair damaged parts and to realign the transfer rod, it was necessary to modify the transfer rod to make it more robust. It was not feasible to replace the screws with rounded heads with flat-head screws since the through holes for the screws were actually slots necessary for the positioning and alignment of the transfer rod. The solution that was implemented was to cover the round screw heads with a flat plate so as to provide a smooth surface to strike the three bearings on the support block. To further improve the transfer assembly, the leading edge of this flat plate was angled so as to make the process of rolling onto the support

block easier. Figure A.1 on p. 81 shows the part that was constructed and installed on the transfer rod. Also, the figure roughly shows how the part covered the round screw heads. Approximate dimensions of the part are also included. Not shown in this figure are a number of small holes and channels that were cut for the purpose of providing gas relief for the part. This cover plate was constructed of aluminum in order to keep the weight as low as possible. While aluminum is not normally used in ultra-high vacuum parts, in this case it was deemed acceptable since the part would never be heated above room temperature.

The installation of this cover plate significantly improved the sample transfer process. Since this part was installed, and the transfer rod last realigned, no serious problems associated with transfer rod misalignment have occured, at least to the time of the writing of this thesis.
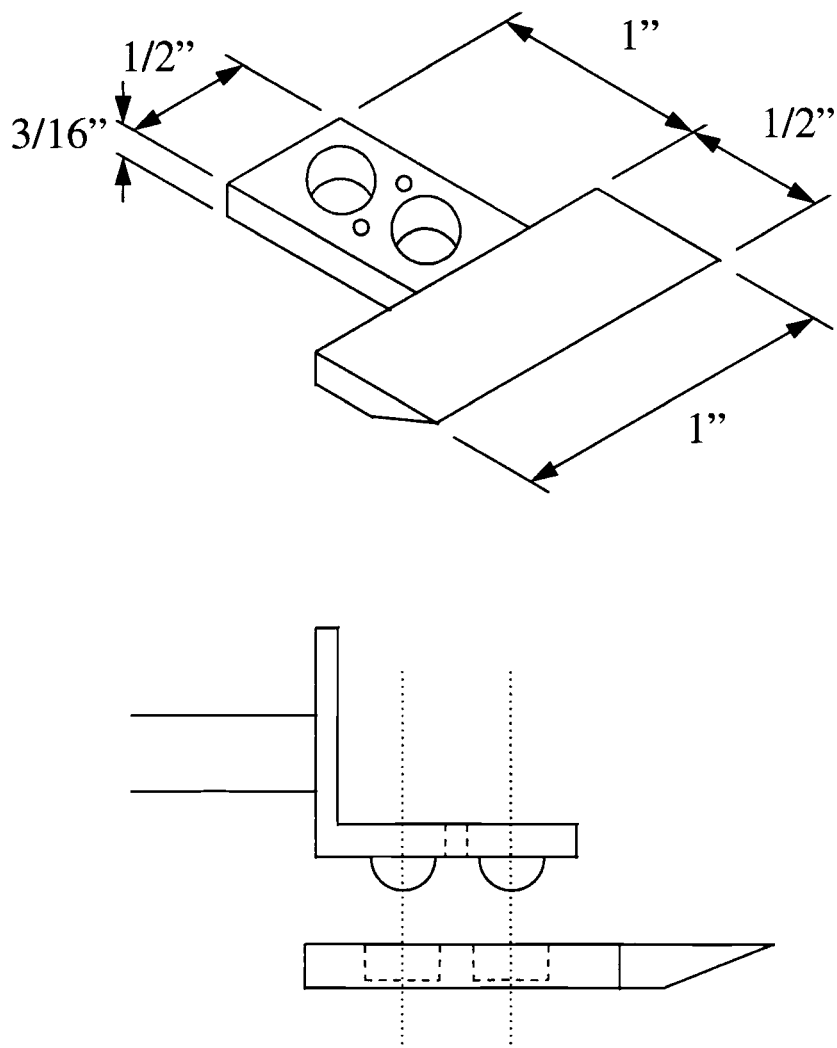
Figure A.1. Shown is the cover plate installed on the magnetic transfer rod to cover the round-headed screws in the sample transfer rod. Dimensions given in the figure are *approximate*. Also shown is the scheme by which the cover plate was installed on the transfer rod.

APPENDIX B

SAMPLE PREPARATION AND OPERATIONAL PROCEDURES

B.1   SUBSTRATE AND SAMPLE BLOCK PREPARATION

B.1.1   SAMPLE BLOCK PREPARATION

Prior to use in an ultra-high vacuum system, all parts and materials must be chemically and physically prepared so as to prevent contaminating the vacuum equipment. The preparation of sample substrates and the sample blocks that hold these substrates during growth is particularly important. The importance of the preparation of the sample substrate is obvious; improperly prepared or contaminated substrates will result in poor quality epitaxial films and could possibly contaminate the vacuum chamber. Of almost equal importance is the preparation of the molybdenum blocks that are used to hold substrates during growth. During growth, these blocks are heated to high temperatures. If not cleaned properly, the blocks will contaminate the deposited films and the growth chamber. In this section the chemical and physical preparation of the molybdenum sample blocks will be discussed. This is a topic which unfortunately has been well researched by this author. There are two basic stages in the preparation of a Mo block for growth: chemical cleaning and etching, and degassing.

The first stage in preparing a sample block is chemical cleaning and etching. The block must be chemically cleaned to remove as much unwanted material as is possible. Common materials that need to be removed from these blocks are deposited materials such as Ga, As, GaAs, and GaN as well as the various alloys of these materials with residual or excess indium which is used to mount the sample

substrates on the Mo blocks. An enormous amount of time and energy can be saved in the chemical cleaning processes if these common materials which build up in repeated use are mechanically removed from the block as best is possible. No effort has ever been made to scrub the blocks by hand using some type of soap solution; the risks of introducing very difficult to remove contaminants far exceed the benefits that this might provide. One cleaning technique that works well is to heat the Mo blocks on a clean hot plate to a temperature sufficient highly to melt indium and to scrape the block with a chemically prepared razor blade. This will remove large amounts of indium and some of the build up of the commonly deposited materials. Another procedure that has provided limited success is to mechanically scrub the blocks using a chemically prepared test-tube brush and deionized (D.I.) water.

Once the macroscopic build-ups of material are removed as best is possible, the Mo blocks may be chemically cleaned and etched. The chemically cleaning procedure is designed to remove any oils or organic materials that may have contaminated the block. While used for a molybdenum part in this case, this cleaning procedure may be used for almost any metal part. The first step in this procedure is to place the block is a clean beaker and to fill well above the height of the Mo block with 1,1,1-trichloroethane (TCA). This beaker and block should be subjected to at least 10 minutes of ultrasonic agitation. After completion of the ultrasonic agitation, the block should be removed from from the TCA. During the remainder of the process, the block should only be handled with Nalgene tools. The block should be rinsed thoroughly with acetone or methanol and should then be placed in a beaker of acetone. Special care should be taken in each transfer from a used and contaminated reagent to a new beaker of reagent to avoid cross contamination. This beaker of acetone should be subjected to at least 10 minutes of ultrasonic agitation. Upon completion of this agitation, the block should be removed from the acetone and rinsed with Methanol. After 10 minutes of ultrasonic agitation in Methanol, the block should be rinsed with D. I. water and subjected to 10 minutes of ultrasonic agitation in a beaker of fresh D. I. water. Note that it is important

to always use fresh D. I. water as it the quality of this purified water will decay quickly in air. If any observable discoloration of the reagents is observed at any stage of the above procedure that step of the cleaning process should be repeated until no further discoloration can be observed. It is also advisable, in general, to start again with the TCA if such discoloration is observed in the later stages. This is especially a good idea when cleaning parts having small features such as screw holes, grooves, etc.

During this process fresh class 100 quality latex gloves should be worn at all times. Special care must be taken to avoid contact of the gloves with the reagents and the Mo block as latex is readily soluble in all of the reagents used in this procedure. All materials and reagents should be disposed of properly. Only Nalgene beakers should be used with the Mo blocks in the ultrasonic bath since glass beakers are commonly chipped and fractured. All beakers and tools should be appropriately cleaned before use in this cleaning process.

Next, it is necessary to chemically etch the molybdenum block. A number of different etches for molybdenum are recommended in various texts and publications. The exact etch that is chosen should depend on the contaminants anticipated to be present on the block. In general, an etch should be chosen that aggressively attacks the contaminant materials and mildly attacks the molybdenum. It has been found, that for blocks that are badly coated with deposited materials, that etching first with an aggressive etch and then with a slower polishing etch works well to prepare the sample blocks. For blocks that have only minor contamination or relatively little build-up, it is likely sufficient to use only the polishing etch that will be presented.

An etch that has been found to work well for badly coated sample blocks is a 1:1:1 solution of HCl, HNO_3, and D. I. water. This etch should be prepared in a clean glass beaker submerged in an ice bath. The glass beaker is necessary since strong etches involving HNO_3 will etch Nalgene and other plastics. The solution should be prepared by adding HNO_3 to D. I. water, and then HCl to the previous mixture. The reagents should be mixed *very slowly*. Particular care should be exercised when HCl is added to either water or H_2O_2, since if heated, Chlorine gas

can be readily evolved. Once prepared, the block should be etched in the solution. The length of etch will be determined by the amount of material to be removed. If left in the etch to long, this etch will cause pits on the block surface. As a rule of thumb, the block should not be left in the etch for more than 1 minute. After etching, the block should be quenched by dipping in successive baths of D. I. water. If flaking of material from the block is observed, the block should be placed in a clean beaker filled with D. I. water and ultrasonically agitated for at least 10 minutes. If necessary, this etch may be repeated; however, this etch should be used conservatively to prevent pitting of the Mo block surface. If only minor amounts of material or spots remain after this etch, the polishing etch below should be used. If the above etch is found to be too weak, the amount of water may be reduced. This etch has been used with no water at all; however, with less water, more care must be taken in the preparation and mixture of the etch. Also, the etch will tend to be more exothermic when less water is used.

A nice polishing etch for the molybdenum blocks is a 1:1:1 mixture of HCl, H_2O_2, and D. I. water. This etch must be prepared and used under an ice bath to prevent the evolution of Chlorine gas. The etch should be prepared by adding H_2O_2 to water and then slowly adding HCl to the mixture under an ice bath. Once prepared, the block may be etched in this solution for 30 to 60 seconds. Following the etch, the block should be quenched by dipping in successive baths of D. I. water. If this etch is found to be too weak, the amount of water may be reduced as above. Likewise, the same considerations must be given for the difficulty of the preparation and the strength or rate of the etch.

If the mixture is removed from the ice bath, this etch will become too fast to be used on vacuum parts. Also, if this etch is used at too high of a temperature, the Mo blocks tend to be left with a dark green or blue stain. This stain has been removed in a number of different ways. Recommended methods of removal are boiling in D. I. water and employing other polishing etches. When used properly, both of these etches have been found to be effective at removing the blue and dark green stains or discolorations that tend to build up on Mo blocks.

The Mo blocks should be dried by blowing with filtered nitrogen gas. Once blown dry, the blocks may further be dried on a clean hot plate that is warm to the touch. If the blocks are excessively heated on the hot plate while drying, they will become badly discolored due to oxidation. Also, the blocks should be stored under vacuum to prevent oxidation in air. This completes the chemical preparation of the molybdenum blocks.

Once the Mo blocks have been sufficiently cleaned by chemical procedures, they must be outgassed in the vacuum environment before being used for growth. It has been found that these blocks should left in the introductory chamber of the MBE system for an extended period of time so that as much outgassing as possible will occur outside of the growth chamber; one day should be taken as an absolute minimum. After the blocks are suitably outgassed in the introductory chamber and then inserted into the growth chamber, they should be outgassed at 100°C until the outgassing of water significantly subsides. Once outgassing at this level subsides, the block should be slowly ramped to a temperature of at least 700°C. During this rampup, significant gas burst should be expected for water, oxygen, carbon monoxide, carbon dioxide, and possibly arsenic. If these gas bursts occur, the rampup should be paused until the pressure significantly subsides. Typically, only the oxygen and carbon monoxide gas bursts will be of significance. The Mo block should be outgassed at 700°C for at least 6 to 8 hours. This may need to be extended if the block is still outgassing after that time. Also, higher temperatures may be necessary if warranted by the growth experiments. Once this is completed, the block may be ramped down to room temperature. The molybdenum block should then be ready for use as a sample holder.

B.1.2 SUBSTRATE HANDLING PROCEDURES

B.1.2.1 SUBSTRATE CLEAVING. The GaAs substrates that have been used for growth to this point in time have been purchased as "Epi-ready" substrates, that is no additional chemical preparation has been necessary for these substrates. The particular Mo blocks and substrate heater that are used with the OSU MBE

system are capable of accommodating 3 inch circular substrates. Substrates of this size are not practical however. Typically, epitaxial films are deposited onto substrates that were attained by cleaving 2 inch circular GaAs Epi-ready substrates into 4 equal pie shaped pieces. Each piece may then be used in different growth experiments.

The GaAs substrates are cleaved by a straight-forward procedure. First, a surface upon which to cleave the substrates must be prepared. It has been found that large specimens are much easier to cleave when supported by a soft or spongy surface. A suitable surface may be attained by wrapping approximately .25 to .50 inches of ordinary lab paper towels in new aluminum foil. The foil may then be cleaned by repeatedly rinsing the surface with TCA, acetone, methanol, and DI water. Further, the surface should be wiped using clean room wipes at each stage. After being thoroughly dried, this surface will serve well for cleaving samples.

A GaAs substrate should be placed, Epi-ready surface up, on the prepared surface. It has been found that any substrate placed polished side down will no longer be suitable for MBE growth. The substrate and all cleaved pieces should be handled using the most delicate tweezer procedures. Also, the cleaved pieces should always be stored in clean Flouroware carriers or their equivalent. Once placed on the prepared surface, a small scratch can be made on the edge of the substrate using a clean diamond scribe. This scratch should be very short, approximately one sixteenth of an inch and oriented perpendicular to either the [110] flat or [1$\bar{1}$0] flat. It will be necessary to refer to the specifications sheet for each individual wafer to determine the crystallographic orientation by using the flats; not all wafers come with the US style of flats. Furthermore, whenever possible, the scratch should be made at a round polished edge as this edge is stronger and weakening the substrate at this point is more critical. It may be necessary to scratch the surface several time in the same location to cause enough damage to allow cleaving of large specimens.

Once the substrate has been scratched, it is then ready to be cleaved. It is best at this point to move the substrate away from prepared surface and to flatten the foil surface by using a clean petri dish or a clean Aluminum block. This helps

to assure that the wafer is evenly supported by the spongy surface. The wafer may then be returned to the smoothed part of the prepared surface and cleaved using a diamond scribe. To cleave the substrate, the point of the diamond scribe should be placed just beyond the end of the scratch that was made away from the edge of the wafer. A controlled amount of force should be applied directly downward. For large samples, the wafer should cleave easily. The pieces should be separated immediately and any GaAs flakes or chips should be blown away using filtered nitrogen gas. The samples may then be cleaved again as necessary or stored. It is advisable to use one diamond scribe for scratching the surfaces and another for cleaving. This will help to prevent the diamond tip in the scribe used for cleaving from being damaged.

B.1.2.2 <u>SUBSTRATE MOUNTING AND REMOVAL</u>. Once a GaAs substrate is suitably cleaved, it may then be mounted to the Mo sample block. The Mo sample block has a flat surface that will be covered with indium. The indium holds the substrate in place by means of surface tension alone during growth experiments.

The Mo sample block should first be placed on a clean aluminum block on a hot plate. The aluminum block is used because it can be more thoroughly cleaned that the hot plate. The aluminum block should be placed in a corner of the hot plate and the hot-plate should be rotated 45 degrees from its normal orientation so that the Mo block can be accessed with a minimal amount of reaching over the hot plate. The hot plate should be set to approximately 75% of its maximum. After 15 to 20 minutes, the Mo block should be almost hot enough to melt indium. If the block has been used in previous growth runs, it will be a good idea to scrape the surface of the block with a clean sharp razor blade before mounting the substrate; deposited material will easily scrape away as a powdery or flaky material. The block should be blown clean with dry nitrogen before proceeding. If this cleaning procedure is not followed, then the Mo block will develop a significant buildup of deposited material on the surface with a pitted area in the center where the substrates are located.

A medium-sized piece of high purity indium from the materials stock should be placed in the center of the Mo block. The temperature should be gradually increased until the indium melts. It is important not to overheat the block since (1) the Mo block oxidizes very quickly in air when heat, and (2) the indium will oxidize rapidly, causing it to turn green and become sticky. Once the indium has melted, it may be pushed about on the Mo block surface using the special ladling tool that was made for this purpose. This tool is basically a razor blade holder with a very long handle. A clean,* sharp razor blade should always be used with this tool for it to work effectively. Using this tool, the indium should be spread out evenly and thinly over the surface of the Mo block. Experience teaches the exact amount and thickness of indium that is necessary. A good rule to start with is that the indium should be the thinnest coating possible that hides the various bumps, pits, and scratches in the center of the block. Uniformity of the indium is very important here. Also, care should be taken to minimize the excess indium that is on the surface and the area that this indium covers.

With the indium suitably spread out on the block, the substrate may be placed on the Mo block. The substrate should be held using a pair of stainless steel tweezers. Also, the substrates should always be handled by the round polished edges rather than by the cleaved edges as they are stronger and much less likely to chip or scratch. It is advisable to hold the substrate just millimeters above the heated Mo surface for as long as possible before placing it on the coating of indium. This allows the substrate to be warmed slightly thus reducing the probability of the substrate shattering due to sudden and uneven heating. After allowing the substrate to be heated, the tweezers should be lowered so that the entire back surface of the substrate strikes indium coating at the same instant in time. Attempting to place one edge down and then lowering the sample onto the indium film inevitably results in shattering the substrate due to the uneven heating. It is highly recommended that one pair of stainless steel tweezers be dedicated for the purpose of placing

---

*It is very important that commercially purchased razor blades be chemically prepared by the procedure described in the previous section. Many commercial razor blades are coated with either plastic or wax to prevent corrosion.

substrates onto the indium and extracting the samples from the indium. It will be obvious which side of this pair of tweezers goes to the indium side and which goes to the sample side; molten indium causes the stainless steel tweezers to turn green. Particular care should be taken in this procedure to not allow gloves or sleeve tips to touch the molybdenum block.

Once the sample is placed on the indium, it should be pushed from side to side using a dedicated pair of tweezers. Pressure should be applied to the side of the substrate, not to the top surface of the substrate. Extreme care should be taken not to touch the top surface. When the wafer is pushed to one side, the excess indium should be scraped from the surface using the ladling tool. Then, the wafer should be pushed to the other side and scraping process repeated. When the thickness of the indium is almost correct, it will become difficult to move the wafer around, that is the motion becomes stiff. The wafer should the be centered on the block and all excess indium removed. If the motion becomes too stiff, this is usually an indicator that the indium film between substrate and the Mo block is too thin; this will usually cause non-uniform heating of the sample during growth.

Once the excess indium is removed, the hot plate should be turned off. It has been found that the GaAs substrate will have less oxide to be thermally desorbed in the growth chamber if it is removed from the hot plate rather than allowing it to cool along with the hot-plate. Thus, the hot plate should first be placed next to another hot plate. Then, the aluminum block along with the Mo block can be pushed onto the cool hot plate. Finally, a clean aluminum block should be placed adjacent to the hot puck and the Mo block should be pushed onto the cool aluminum block. After approximately 30 minutes, the block should be cool enough to insert into the introductory chamber. As the last step before inserting the Mo block with the substrate into the vacuum chamber, the Mo block should be blown clean using dry nitrogen gas to remove any dust particles that may have settled as the block was cooling. It is also advisable to inspect the substrate under a microscope just before inserting it into the chamber. Notes should be make of any imperfections in the substrate surface.

To remove a sample from its indium mounting much of the same procedure is followed. First the Mo block with the sample should be placed on an aluminum block in the same geometry as described before. The hot plate should be set to approximately 80% of its maximum output and should be allowed approximately 20 minutes to heat fully. At this power level, the indium should be molten. Using either the specially designed tool or a tweezer with a very blunt edge, pressure may be applied to the side of one of the cleaved surface of the samples. The sample should require a small amount of force to break free and almost no force to move it afterwards. Once broken free, the sample should be pushed to the edge of the Mo block so that one of the round polished edges overhangs slightly. The sample may then be picked up with the same pair of tweezers that was used to place it on the Mo block. Care should be taken to see that the correct side of the tweezer is turned to the indium coated back surface of the sample. After lifting the sample from the Mo block, it should be moved away from the hot plate and held directly over a clean surface for 30 to 60 seconds. This allows the sample to cool in air before it is placed in its Flouroware holder. The clean surface is necessary in case the sample is dropped in this period of time. After cooling in air for 30 to 60 seconds, the sample should be stored in a Flouroware container. After the sample is safely stored, the heated Mo block should be scraped clean with the ladling tool. At this point, another substrate may be loaded or the block may be cooled by the procedure above and returned to the vacuum chamber.

Whenever working with samples or substrates, especially GaAs, safety goggles should always be worn since large samples are very prone to shattering. Also, suitable class 100 clean room gloves should be worn for all operation involving samples, substrates, source materials, or the Mo blocks. Furthermore, it is highly advised that loose cuffs on the sleeves of clean room garments be restrained using tape or rubber bands to keep them out the way.

B.2 PREPARING AND LEAK-CHECKING THE N$_2$ GAS MANIFOLD

B.2.1 N$_2$ GAS MANIFOLD PREPARATION

When the MBE system was upgraded for ECR-MBE growth of GaN, it was necessary to install a network of valves and gas lines to provide the high purity nitrogen gas to the ECR source. A diagram of the various components that comprise the nitrogen source gas manifold is given is Fig. B.1 on p. 93. As can be seen in the figure, there are a non-trivial number of components to the nitrogen source gas manifold. There has been developed for this manifold a well developed procedure to prepare the nitrogen source gas manifold for delivering nitrogen gas to the ECR source. Furthermore, there is a well developed procedure for preparing the MBE system to accommodate the high pressure of nitrogen gas and for establishing the nitrogen gas flow.

The procedure for preparing nitrogen source gas manifold is as follows. First, a sorption pump should be cooled with liquid nitrogen; whenever possible, the liquid nitrogen should be poured at least thirty minutes before beginning the pump down of the source gas manifold. After the sorption pump is sufficiently cooled, the main roughing manifold should be pumped out. The pressure of the main roughing manifold should be monitored throughout using the convectron gauge located near the sorption pumps. This gauge will measure pressures as low as 1.0×10^{-4} Torr; below this level, the gauge simply reads as zero.

After the main roughing manifold has been pumped below the convectron's zero, the valves on the nitrogen source gas manifold should be slowly opened, one at a time. After opening each valve, the user should wait until the pressure has dropped near to the zero level of the convectron gauge. The order in which the valves are to be opened is shown in Fig. B.1 on p. 93. The pressure regulator should remain fully relieved during this procedure, that is with no pressure applied to the source gas manifold. Also, the main valve at the nitrogen gas cylinder should remain closed through this procedure. The source gas manifold is considered ready for use after the pressure in all sections of the source gas manifold are pumped below the zero
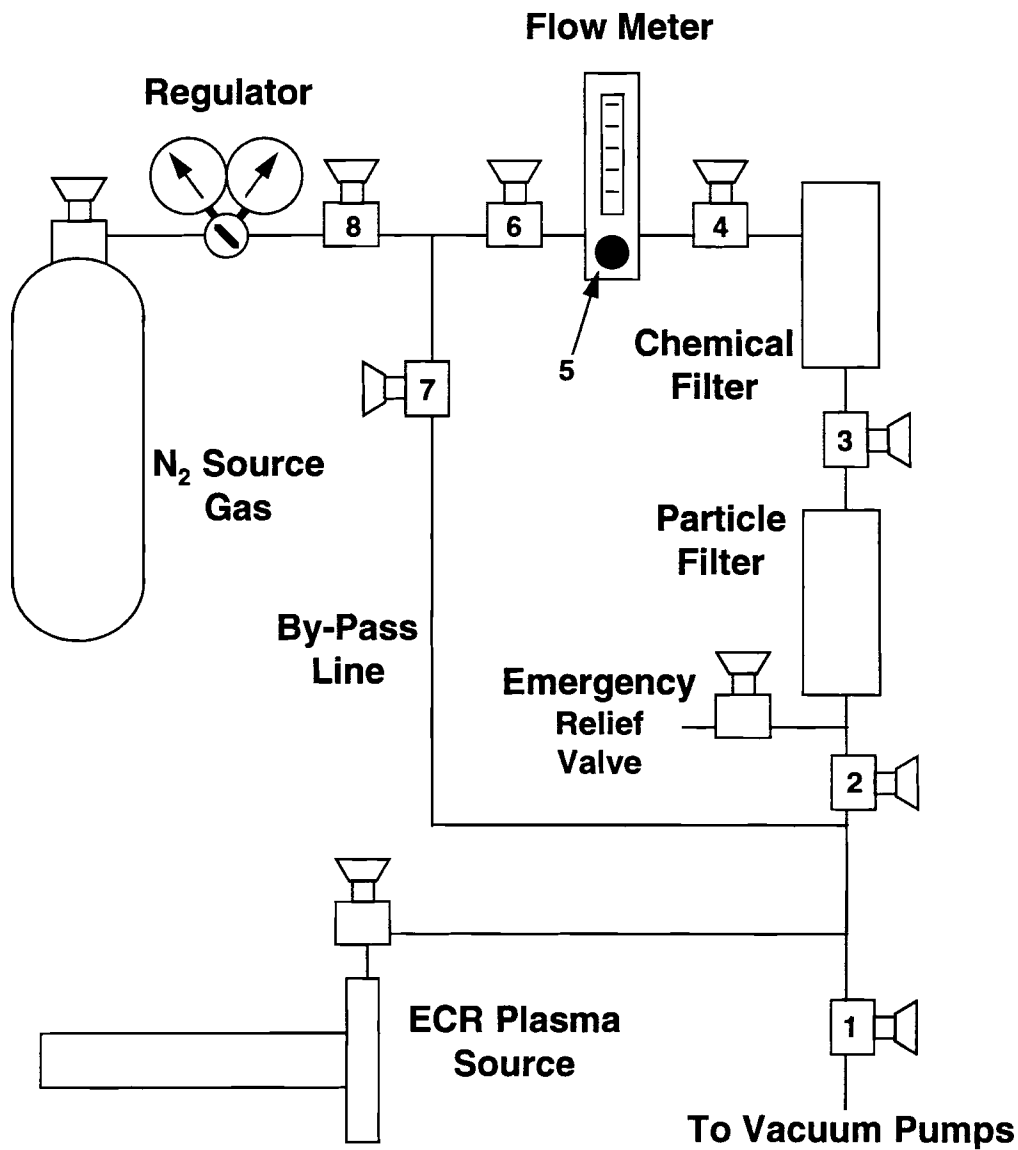
Figure B.1. Shown are the various components that comprise the nitrogen source gas supply line. The numbers indicate the order in which the valves should be opened while preparing the nitrogen source gas manifold for use.

level of the convectron gauge. If the sorption pump that is used for this procedure has not been recently regenerated, the time required to pump the entire manifold below the zero level of the convectron gauge may be excessively long. The time required to pump down can be significantly reduced by closing the valve separating the sorption pump from the roughing manifold and opening the valves between the CT-100 cryo-pump and the roughing manifold. This procedure should be avoided unless absolutely necessary as this will force more frequent regenerations of the CT-100 cryo-pump.

In order to introduce the flow of nitrogen gas into the MBE system, the following procedure is used. First, the nitrogen source gas manifold must be prepared as described above. Next, the valves numbered 1, 5, and 7 in Fig. B.1 should be closed in the order listed. Once these valves are closed, the needle valve separating the ECR plasma source from the nitrogen source gas manifold should be fully opened. The RGA should be turned off since the nitrogen pressure levels are too high for it to operate without being damaged. The growth pressure interlock should be overridden to always be satisfied and the ion gauge emission currents should be set to the minimum setting of 0.1 amp. The gate valve for the CT-8 cryo-pump should be fully opened and the gate valve for the 500 liter/sec ion pump should be fully closed.

Once these operations are complete, the nitrogen gas may be introduced into the chamber. To do this, first, the main valve on the nitrogen gas cylinder is opened. The pressure regulator should be set for 10 psi (gauge). Next, the flowmeter valve is opened and set so that the steel ball is at position 50. This position should deliver a nitrogen gas flow rate of 26 standard cubic centimeters per minute (sccm). At this point, the nitrogen source gas will be flowing into the MBE growth chamber through the ECR source. The pressure should steadily rise to approximately 1.0×10^{-5} Torr. When the pressure approached this level, the CT-8 cryo-pump gate valve should be partially closed to attain the desired chamber pressure. For all of the samples grown for this thesis, this condition has been 2.0×10^{-4} Torr as measured by ion gauge #2 or 2.2×10^{-4} Torr as measured by ion gauge #1. Fine adjustments will

need to be made to the CT-8 cryo-pump gate valve and the flowmeter until the pressure stabilizes at the desired flow rate. At this point, the introduction of the nitrogen source gas is complete.

B.2.2 N$_2$ GAS MANIFOLD LEAK CHECKING

The large number of components in the nitrogen source gas manifold makes the leak-checking procedure difficult. The procedure for finding leaks necessarily depends on the size of the leak. For leaks that are sufficiently small or slow, the gas manifold may be opened up to the growth chamber so that the leak-check function of the Quadrapole Mass Spectrometer or Residual Gas Analyzer (RGA) may be used.

The leak-check function of the RGA allows the user to select a particular mass to monitor. In this mode, the RGA will monitor only the selected mass. The RGA will emit a tone at a fixed volume but at variable frequency. The frequency of the tone is proportional to the measured partial pressure of the selected mass. That is, for a higher pressure of the selected mass a higher tone is emitted. In the laboratory, flanges or gaskets that are suspected of leaking may be checked by using the RGA and a gas that is not abundant in nature. For example, the area surrounding a flange or gasket may be saturated with helium gas by using a fine tipped spray gun and a bottle of compressed helium. If there is a leak, an increase in the frequency of the tone from the RGA will be heard. It this way, flanges and fittings may be checked for leaks.

The nitrogen source gas manifold may be checked for leaks in this way provided that the leaks are sufficiently slow. First, the gas manifold should be pumped out using one of the sorption pumps on the roughing manifold. Once a sufficiently low pressure has been established, the needle valve separating the ECR source from the nitrogen source gas manifold may be opened. Then the various flanges and fittings may be checked by using a Helium spray gun and the RGA by the procedure above. While checking for leaks by this procedure is usually the fastest method of locating the exact source of a vacuum leak, this is by no means

a fast experiment. The conductance of the nitrogen source gas manifold is quite poor. Therefore, the response time of the RGA to a particular blast of helium will be quite long.

When leak rates are sufficiently high so that the growth chamber cannot be exposed to the leak, the procedure becomes more difficult. First, it is useful to determine what section of the nitrogen source gas manifold is leaking. To do this, the entire nitrogen source gas manifold should be pumped to high vacuum conditions using one of the sorption pumps on the roughing manifold. Once pumped out, all valves on the gas manifold should be closed, starting from the valves closest to the Nitrogen gas cylinder and working towards the roughing manifold. After all valves are closed, the source gas manifold should be left unperturbed for some length of time sufficiently long so that the leaky section of the manifold will gain pressure. A leaky section may be identified by successively opening valves, starting from the roughing manifold and moving towards the nitrogen gas cylinder, and observing the pressure readings after opening each valve. A sudden increase in pressure would indicate a leaky section.

When further localization is needed for a fast leak, a very tedious procedure may be used to locate it. First the nitrogen source gas manifold should be pumped out using a sorption pump. Then, the area surrounding a suspected leak should be saturated with a gas that cannot be pumped efficiently by the sorption pump, such as helium. If there is a leak at the suspected fitting or flange, a rise in pressure may be seen. It should be noted that this is a difficult and tedious method of finding leaks. The pressure rises will be relatively small and the response time of the system will be quite long due to the poor conductance of the nitrogen source gas manifold. However, this method has been used effectively to find leaks in the Nitrogen source gas manifold.

VITA

MARK L. O'STEEN

Candidate for the Degree of

Master of Science

Thesis: MBE GROWTH AND INTIAL NUCLEATION KINETICS OF GaN
ON GaAs (100) SUBSTRATES

Major Field: Physics

Biographical:

Personal Data: Born in Denison, Texas, on March 23, 1971, the son of Jim
and Karen O'Steen.

Education: Graduated from Durant High School, Durant, Oklahoma in May
1989; received Bachelor of Science degree in Physics and Mathematics
from Southeastern Oklahoma State University, Durant, Oklahoma in
May 1993. Completed the requirements for the Master of Science degree
with a major in Physics at Oklahoma State University in December
1995.

Professional Memberships: American Physical Society, Society of Physics Stu-
dents.